UNIVERSIDAD NACIONAL AUTÓNOMA DE MEXICO

MAESTRIA EN CIENCIAS FISICAS
INSTITUTO DE FISICA

THE ROLE OF LONGITUDINAL CORRECTIONS IN B→l ν D* DECAYS AS LEPTON FLAVOR UNIVERSALITY TESTS

TESIS
QUE PARA OPTAR POR EL GRADO DE:
MAESTRO EN CIENCIAS (FISICA)

PRESENTA:
JORGE EMMANUEL CHAVEZ SAAB

TUTOR PRINCIPAL:
DR. GENARO TOLEDO SANCHEZ
INSTITUTO DE FISICA UNAM

COMITE TUTOR:

EDUARDO PEINADO RODRIGUEZ
INSTITUTO DE FISICA UNAM

ALEXIS ARMANDO AGUILAR AREVALO
INSTITUTO DE CIENCIAS NUCLEARES UNAM

CIUDAD UNIVERSITARIA, CD. MX, 16 DE NOVIEMBRE DEL 2018

A mis padres y a mi hermano.

Agradecimientos

Quiero expresar mi profundo agradecimiento al Dr. Genaro Toledo Sánchez por todo el apoyo tan cercano y la orientación que me ha brindado para mi formación tanto académica como personal en los últimos años.

Agradezco también al Dr. Eduardo Peinado Rodríguez y al Dr. Alexis Aguilar Arévalo por su valiosa retroalimentación en la realización de este trabajo, asi como al Dr. Genaro Toledo Sánchez, la Dra. Myriam Mondragón Ceballos, el Dr. Roelof Bijker, el Dr. Paul Artur Jens Erler Weber y el Dr. Pablo Roig Garcés por sus aportaciones como sinodales de este trabajo.

Gracias a mis padres por apoyarme económicamente a lo largo de mi formación académica, pero más aún por el apoyo personal que siempre me han dado.

Doy también las gracias a la UNAM por la invaluable oportunidad de haber realizado parte de mi formación en tan prestigiosa casa de estudios, y al CONACYT por el apoyo económico que me ha proporcionado en este periodo.

Resumen

Este trabajo se enfoca en los decaimientos $B \to l\nu D^*$ como pruebas de universalidad de sabor leptónico, los cuales se han vuelto un argumento popular para la justificación de física más allá del modelo estándar ya que experimentos recientes han medido un exceso consistente de productos con sabor tau. Específicamente, se han medido desviaciones con significación estadística de 3.7σ en la razón de tasas de decaimiento $R^*_D \equiv BR(B \to \tau\nu D^*)/BR(B \to l\nu D^*)$. Aquí argumentamos que esta discrepancia puede no ser una señal de violaciones a la universalidad de sabor leptónico, sino que se debe al menos en parte al hecho de que el D^* no es un estado asintótico y los cálculos teóricos deben hacerse con el proceso completo que incluye a sus productos – ya sea $D\pi$ o $D\gamma$. Trabajamos únicamente con el canal $D^* \to D\pi$ y mostramos que el grado de libertad longitudinal del D^*, el cual se vuelve disponible una vez que éste se toma fuera de capa de masa, introduce una corrección considerable al hacer interferencia con el grado transversal. Encontramos una nueva razón $R_{D\pi} = 0.275 \pm 0.003$, donde la incertidumbre se hereda de la de la medición de los factores de forma que describen al vértice de QCD. Al comparar con la razón $R_{D\pi}$ en vez de R_{D^*}, la brecha con los últimos resultados de LHCb se reduce de 1.1σ a 0.48σ, mientras que la de los últimos resultados de Belle se reduce de 0.42σ a 0.10σ, y con el promedio mundial de 3.7σ a 2.1σ. Ya que el desacuerdo con los resultados más recientes parece desaparecer por completo, argumentamos que el problema de $R_{D\pi}$ podría ser resuelto sin la necesidad de recurrir a ningún tipo de física más allá del modelo estándar. Ya que todo el análisis de datos se ha hecho asumiendo el decaimiento original a tres cuerpos, incluyendo el cálculo de los factores de forma para el vértice de QCD, nuestro resultado debe considerarse aún como una aproximación. Por lo tanto, hacemos también un planteamiento de los siguientes pasos a seguir y las consideraciones adicionales que deberían hacerse una vez que el D^* sea tomado fuera de capa de masa. Resaltamos que un análisis del decaimiento

a cuatro cuerpos sería extremadamente útil para refinar nuestro resultado de $R_{D\pi}$, y posiblemente cerrar la brecha con el promedio mundial aún más.

Summary

This work focuses on the semileptonic decays $B \to l\nu D^*$ as tests for lepton flavor universality, which have become a popular argument for physics beyond the standard model in recent years after experiments started consistently detecting an excess of tau products. Specifically, the ratio of tau to light lepton products, $R_{D^*} \equiv BR(B \to \tau\nu D^*)/BR(B \to l\nu D^*)$, has been found to deviate by 3.7 σ from the standard model prediction. We argue that this discrepancy may not be a sign of lepton flavor universality violation, but is due at least in part to the fact the D^* is not an asymptotic state and the theoretical calculations should be done with the complete process including its daughter particles - either $D\pi$ or $D\gamma$. We work only with the $D^* \to D\pi$ mode and show that the longitudinal degree of freedom of the D^*, which becomes available when it is taken off shell, although small by itself, introduces a sizable correction when interfering with the transversal degrees of freedom. We find a new ratio of $R^{\mu}_{D\pi} = 0.275 \pm 0.003$, where the uncertainty comes from the uncertainty of the form factors parameters. Comparing against $R_{D\pi}$ reduces the gap with the latest LHCb result from 1.1σ to 0.48σ, while the gap with the latest Belle result is reduced from 0.42σ to just 0.10σ and with the world average results from 3.7σ to 2.1σ. Since the disagreement with the latest results is completely gone, this might indicate that the R_{D^*} problem could be solved without the need of lepton flavor universality violation or any form of physics beyond the standard model. Since all the data analysis has been done assuming only a three body decay, including the calculation of the form factors that we use for the QCD vertex, our answer should still be considered an approximation. Therefore, we also lay the groundwork for other considerations that should be made once the D^* is taken to be off shell and point out that a proper four body analysis of the experimental results could be used to refine our result for $R_{D\pi}$, and possibly close the gap with the world average even further.

Contents

Chapter 1

Introduction

The assumption of lepton flavor universality (LFU) states that the rules of physics are invariant under any exchange between the three families of leptons, and is closely tied to the gauge invariance of the standard model (SM). Each of the lepton families is assumed to have exactly the same coupling to gauge bosons, so that processes related by flavor symmetry involve the same types of diagrams and the only differences that arise are of kinematical origins. Put simply, the couplings of each of the families must all be the same, but their masses are allowed to differ. Because new theories of physics beyond the standard model often involve the breaking of gauge symmetries, the search for LFU violation has gained significant relevance in recent years. In this work we focus on the search for LFU violation in the weak sector, namely differences in the weak coupling constant among lepton flavors.

The weak sector is where these searches have returned the most interesting results, and can be explored through semileptonic decays of heavy mesons of the form $M_1 \to l^+ \nu_l M_2$. The reason for requiring a heavy meson is to enable the production of τ particles, for which we need a quark-level transition with a large mass difference, ideally $b \to c$. Thus, we naturally arrive to the processes of the form $B \to l^+ \nu D^{(*)}$ that are central to this work. This encompasses two different cases that are treated equivalently:

$$B^0 \to l^+ \nu D^{(*)-}, \text{ if the spectaror quark is } d, \text{ and}$$
$$B^+ \to l^+ \nu D^{(*)0}, \text{ if the spectaror quark is } u,$$

as well as all charge-conjugate modes. These processes have a single tree-level diagram, shown in Fig. 1.1, where the emission of the lepton-neutrino

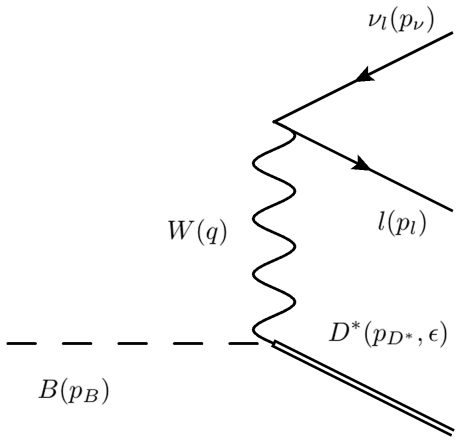

Figure 1.1: Tree-level diagram of the $B \to l\nu D^{(*)}$ process.

pair happens through a virtual W boson. Therefore, we can use this process to probe the coupling of each lepton-neutrino family to the weak sector. Because the decay widths are proportional to several constants with relatively large uncertainties, it is convenient to make the comparison between different flavors by considering the ratio

$$R_{D^{(*)}} \equiv \frac{Br(B \to \tau^+ \nu_\tau D^{(*)})}{Br(B \to l^+ \nu_l D^{(*)})}, \quad l = e, \mu,$$

where the overall factors cancel out. This is the quantity that is expected to reflect the lepton flavor universality property of the process, and is often stated as independent of the choice of l due to the small mass difference relative to the τ mass. The standard model predicts values for $R_D^{SM} = 0.300(8)$ [1] and $R_{D^*}^{SM} = 0.252(3)$ [2] that are based solely on the different masses of the leptons, and these values are compared to experimental results as a form of precision test for lepton flavor universality.

Historically, the experimental measurements of the R_D and R_{D^*} ratios have controversially but consistently pointed towards higher values than the standard model prediction, prompting the possibility that an effect of LFU violation is being observed. The first measurements were reported by the BaBar collaboration in 2013, and indicated a disagreement with the standard model of 2.0 σ for R_D and 2.7 σ for R_{D^*} [3, 4]. Later results by the

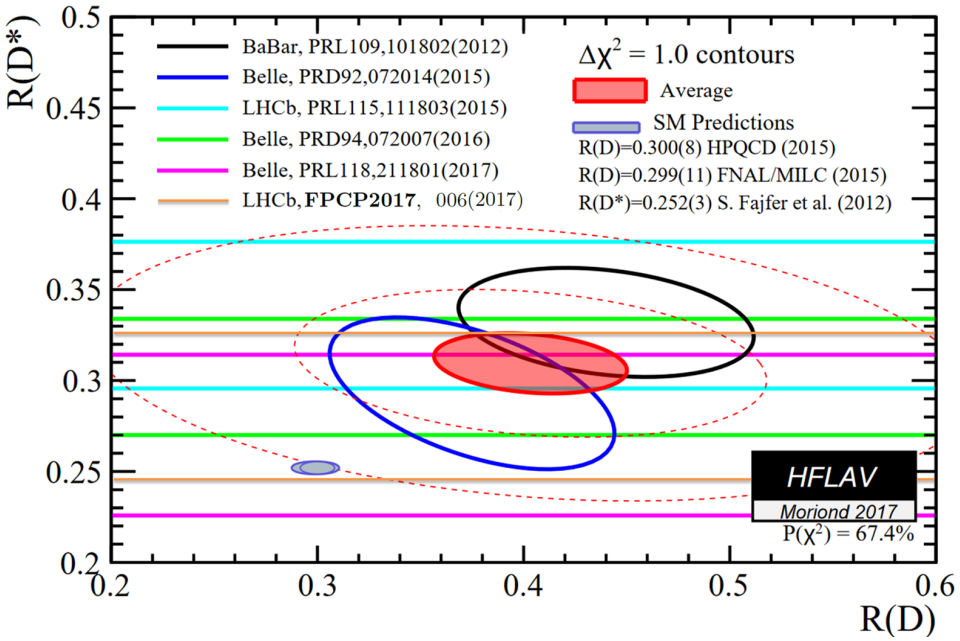

Figure 1.2: Summary of the R_D and R_{D^*} measurements performed by different collaborations. The shaded red area represents the average of all experiments, and the shaded blue area is the standard model prediction. Image produced by [12].

Belle [5, 6] and LHCb [7] collaborations were published in 2015 and were in agreement with BaBar. All of these experiments chose to reconstruct the product τ's only through leptonic decays, excluding the cases with hadronic decays so that both $B \to \tau\nu_\tau D^{(*)}$ and $B \to l\nu_l D^{(*)}$ would be identified through the same daughter particles. However, in 2017 the LHCb [8, 9] and Belle [10, 11] collaborations published their latest results, which included hadronic channels for the τ detection, and significantly closed the gap on R_{D^*} to 0.9 σ and 0.4 σ, respectively. Nevertheless, the world-average for all the experiments is still at a 3.5 σ disagreement with the standard model prediction, and it is this disagreement that we will focus on in this work. A visual summary of all the measurements performed is provided by Fig. 1.2, and the exact values reported are shown in Table 1.1.

In this work we are concerned solely with the ratio R_{D^*} and not R_D, and we propose a method to bring the standard model prediction closer to experimental results that is based on considering the longitudinal degree

Table 1.1: Results on R_D and R_{D^*} reported by various experiments.

	R_D	R_{D^*}
BaBar[3, 4]	$0.440 \pm 0.058 \pm 0.042$	$0.332 \pm 0.024 \pm 0.018$
Belle [5]	$0.375 \pm 0.064 \pm 0.026$	$0.293 \pm 0.038 \pm 0.015$
Belle [6]		$0.302 \pm 0.030 \pm 0.011$
LHCb[7]		$0.336 \pm 0.027 \pm 0.030$
Belle[10, 11]		$0.270 \pm 0.035^{+0.028}_{-0.025}$
LHCb[8, 9]		$0.291 \pm 0.019 \pm 0.029$
Average[12]	$0.407 \pm 0.039 \pm 0.024$	$0.306 \pm 0.013 \pm 0.007$
Theoretical	0.300 ± 0.008[1]	0.252 ± 0.003[2]

of freedom of the D^*. Our calculations are based only on a more detailed analysis using the standard model and do not assume any LFU violation, nor do they rely on any other form of new physics. As experimental precision continues to increase, and with the upcoming Belle 2 experiment expected to have a 75% increase in its precision for the R_{D^*} measurement [13], it will be increasingly important to have a solid and more rigorous standard model calculation to compare the results to, which is what has inspired this work. Specifically, we take into account the fact that the D^* is an unstable particle, and thus it is never detected directly but through its decay into daughter particles, which are most commonly a $D\pi$ pair. Therefore, what the experiments observe is not a three-body decay and it is not appropriate to compare the results with the ratio R_{D^*}, but with a new ratio $R_{D\pi}$ obtained from the whole four-body $B \to l\nu_l \pi D$ decay. In this new process, the D^* becomes an off-shell particle, which enables its longitudinal degree of freedom. These are the longitudinal corrections to the process that we refer to in the title, and which we aim to calculate. Taking the D^* off-shell requires the much harder task of calculating the four-body $B \to l\nu\pi D$ decay instead of the three-body $B \to l\nu D^*$ decay, which is rarely actually done because the longitudinal contribution is thought to be heavily suppressed. However, we will show that the corrections that arise in the ratio are not negligible, in great part due to the large mass difference between the daughter π and D particles, and that they help to considerably close the gap with the experimental data. Therefore, it is more likely that the experiments can be reconciled with the standard model, without the implication of LFU violation.

It should be noted that neutral D^* mesons also exhibit the $D^* \to D\gamma$ decay mode, where the longitudinal corrections that we have mentioned are

absent. Throughout this work we neglect this mode and work only with the $D^* \to D\pi$ mode, so our results should be considered a better description for experiments using only charged D^* mesons which exhibit $D^* \to D\pi$ with a branching ratio of 98.4% [14]. Experiments that use only charged D^* mesons are the 2016 results by Belle [6] as well as all LHCb experiments [7–9]. Other Belle measurements [5, 10, 11] and BaBar results [3, 4] use both charged and neutral particles, and report a single value for R_{D^*} assuming the result makes no distinction.

In order to achieve our goal, we will begin with a brief review in chapter 2 of all the basic elements of quantum field theory that we will need in order to set up the theoretical framework of our calculations, as well as the general characteristics of the standard model. In chapter 3, we present a thorough analysis of the longitudinal corrections and the $B \to l\nu D^*$ process as a whole, and go over the technical aspects needed to calculate the decay width. Finally, in chapter 4 we present our results and discuss the implications they have, and also propose some new directions that future research in this subject could follow in order to further refine these results.

Chapter 2

Quantum Field Theory and the Standard Model

In this chapter we present a brief overview of all the basic elements of the standard model and quantum field theory needed in order to study the $B \to l\nu D^*$ process. Although we only go into detail for topics that are pertinent to this decay, we attempt to describe these ingredients in as much generality as possible, leaving more detailed insights into the particular case of the $B \to l\nu D^*$ process for chapter 3. We begin by describing the basic aspects of the Dirac field in section 2.1 and of the vector field in section 2.2. In section 2.3 we go over gauge symmetries and the couplings of leptons to gauge bosons, deriving the Feynman rules along the way. We put all these ingredients together in section 2.4, where we present a summary of all the particles and interactions of the standard model, and then give a description of mesons based on the quark model in section 2.5. Finally, we discuss the phase space kinematics of three- and four-body decay processes in section 2.6, and present the integration method that we will use.

2.1 Fermions

The group of fermions consists of all half-integer spin particles, and includes everything that we typically conceive as matter. In quantum relativistic mechanics, a fermion is described by a four-tuple of complex numbers, called a spinor, which takes some value at each point of space and time. The evolution of a spinor $\Psi(x)$ for a spin-1/2 particle of mass m is determined by

the Dirac equation:

$$(i\gamma^\mu \partial_\mu - m)\Psi(x) = 0,$$

where γ^μ are the Dirac gamma matrices, which are 4x4 complex matrices chosen to satisfy $\{\gamma^\mu, \gamma^\nu\} = 2g^{\mu\nu}$, with $\{\cdot,\cdot\}$ denoting the anticommutator and $g^{\mu\nu} \equiv diag[1,-1,-1,-1]$ the flat space metric tensor. This definition of the gamma matrices is such that $S^{\mu\nu} \equiv \frac{i}{2}[\gamma^\mu, \gamma^\nu]$ forms a valid representation of the Lorentz group generators, which indicate how a spinor transforms under a Lorentz transformation [15].

We also define the left and right components of a spinor as

$$\Psi_L \equiv \frac{1}{2}(1-\gamma_5)\Psi$$

$$\Psi_R \equiv \frac{1}{2}(1+\gamma_5)\Psi,$$

where $\gamma_5 \equiv i\gamma^0\gamma^1\gamma^2\gamma^3$ is hermitian and has the property $\{\gamma_5, \gamma^\mu\} = 0$. This allows us to decompose any spinor as $\Psi = \Psi_L + \Psi_R$.

The Dirac equation can also be obtained from the Lagrangian

$$\mathcal{L}_D = \bar{\Psi}(i\gamma^\mu \partial_\mu - m)\Psi$$

if we consider Ψ and its adjoint spinor $\bar{\Psi}$ as independent variables. In order for the Lagrangian to be a Lorentz scalar, the adjoint is defined as

$$\bar{\Psi} \equiv \Psi^\dagger \gamma^0.$$

This makes it so that $\bar{\Psi}\Psi$ is a Lorentz scalar, while quantities like $\bar{\Psi}\gamma^\mu\Psi$ transform like a vector and $\bar{\Psi}\gamma^\mu\gamma^\nu\Psi$ like a tensor of rank 2.

In addition to Lorentz transformations we also have the parity transformation $(x^0, \vec{x}) \mapsto (x^0, -\vec{x})$. When acting on a spinor, this may be implemented in several ways. In the Weyl basis [16], one has

$$\hat{P}\Psi = \eta_P \gamma^0 \Psi,$$

where η_P can be either +1 or -1 and is known as the parity of the particle. The scalar form $\bar{\Psi}\Psi$ and the vector form $\bar{\Psi}\gamma^\mu\Psi$ behave as one would expect under parity. That is, the scalar is unaffected by it while the vector has the sign of its spatial components switched. On the other hand, quantities like $\bar{\Psi}\gamma_5\Psi$ are called pseudoscalars because they transform like scalars under Lorentz transformations but gain a negative sign under parity, and quantities

like $\bar{\Psi}\gamma_5\gamma^\mu\Psi$ are called pseudovectors or axial vectors because they transform like vectors under Lorentz transformations but under parity all components switch sign, not just the spatial ones. The parity operator also exchanges the left and right components of a spinor:

$$\hat{P}\Psi_L = \eta_P\Psi_R \qquad \text{and} \qquad \hat{P}\Psi_R = \eta_P\Psi_L.$$

Any solution to the Dirac equation can be written in terms of four types of normal modes, namely:

$$\begin{aligned}\Psi_p^1(x) &= u_p^1 e^{-ip\cdot x}\\ \Psi_p^2(x) &= u_p^2 e^{-ip\cdot x}\\ \Psi_p^3(x) &= v_p^1 e^{+ip\cdot x}\\ \Psi_p^4(x) &= v_p^2 e^{+ip\cdot x},\end{aligned}$$

where [17]

$$u_p^s = \frac{m + \gamma^\mu p_\mu}{\sqrt{2(p^0+m)}}\begin{pmatrix}\xi^s\\ \xi^s\end{pmatrix}$$

and

$$v_p^s = \frac{m - \gamma^\mu p_\mu}{\sqrt{2(p^0+m)}}\begin{pmatrix}\xi^s\\ \xi^s\end{pmatrix},$$

with

$$\xi^1 = \begin{pmatrix}1\\0\end{pmatrix}, \quad \xi^2 = \begin{pmatrix}0\\1\end{pmatrix}.$$

The spinors u_p^1 and v_p^1 correspond to a particle and antiparticle of spin up, while u_p^2 and v_p^2 correspond to a particle and antiparticle of spin down. Moreover, the u_p^s and v_p^s spinors satisfy the orthogonally relations

$$u_p^{s_1\dagger}u_p^{s_2} = v_p^{s_1\dagger}v_p^{s_2} = 2p^0\delta^{s_1 s_2}$$

and the spin sum rules

$$\begin{aligned}\sum_s u_p^s u_p^{s\dagger} &= \gamma^\mu p_\mu + m,\\ \sum_s v_p^s v_p^{s\dagger} &= \gamma^\mu p_\mu - m.\end{aligned} \tag{2.1}$$

From this one can derive the free propagator and the Feynmann rules for the Dirac field:

- For an incoming particle of spin s, add the spinor u_p^s
- For an incoming antiparticle of spin s, add the spinor $\bar{v}_p^s$
- For an outgoing particle of spin s, add the spinor $\bar{u}_p^s$
- For an outgoing antiparticle of spin s, add the spinor v_p^s
- For each internal line, add the propagator $\frac{i\gamma^\mu p_\mu + m}{p^2 - m^2}$

2.2 Bosons

The second group of particles, the Bosons, consists of all particles of integer spin, which are typically conceived as force carriers. The standard model contains only one particle of spin 0, which we need not delve into. All other bosons are spin-1 particles which are described by the vector field. The vector field receives its name because it is a four-tuple of complex numbers just like the Dirac field, but under Lorentz transformations its components transform just like the components of a four-vector.

We will begin by analyzing the case of a massless spin-1 particle, which has only two internal degrees of freedom (*i.e.* two spin states). This means that a description using the four components of a vector field has two additional degrees of freedom that are redundant. This redundancy can be addressed by associating into equivalence classes all the configurations of the vector field that differ by a total derivative. That is, for a vector field A^μ we have

$$A^\mu(x) \cong A^\mu(x) + \partial^\mu \theta(x)$$

for any function $\theta(x)$, where the equivalence means that the two configurations represent the same physical state, and we say that the two configurations are related by a gauge transformation. The only free Lagrangian that we can write that is invariant under both gauge and Lorentz transformations is the Maxwell Lagrangian,

$$\mathcal{L}_M = -\frac{1}{4} F^{\mu\nu} F_{\mu\nu},$$

where $F^{\mu\nu} \equiv \partial^\mu A^\nu - \partial^\nu A^\mu$. The equations of motion that result from this Lagrangian are the inhomogeneous Maxwell equations without sources,

$\partial_\mu F^{\mu\nu} = 0$. Any solution to this equation can be decomposed into normal modes of four kinds:

$$A^{\mu}_{k+}(x) = \epsilon^{\mu}_{k+} e^{-ik\cdot x},$$
$$A^{\mu *}_{k+}(x) = \epsilon^{\mu *}_{k+} e^{+ik\cdot x},$$
$$A^{\mu}_{k-}(x) = \epsilon^{\mu}_{k-} e^{-ik\cdot x},$$
$$A^{\mu *}_{k-}(x) = \epsilon^{\mu *}_{k-} e^{+ik\cdot x},$$

where the polarization vectors correspond to a left and right circular-polarized particle and can be taken as

$$\epsilon^{\mu}_{k+} = \Lambda \begin{pmatrix} 0 \\ 1/\sqrt{2} \\ i/\sqrt{2} \\ 0 \end{pmatrix}, \qquad \epsilon^{\mu}_{k-} = \Lambda \begin{pmatrix} 0 \\ 1/\sqrt{2} \\ -i/\sqrt{2} \\ 0 \end{pmatrix},$$

with Λ a Lorentz transformation matrix that maps $(1, 0, 0, 1) \mapsto k$.

This allows us to derive the free propagator and the Feynmann rules for the massless vector field [17]:

- For each incoming particle of polarization $\pm$, add the polarization vector $\epsilon^{\mu}_{k\pm}$
- For each outgoing particle of polarization $\pm$, add the polarization vector $\epsilon^{\mu *}_{k\pm}$
- For each internal line, add the propagator $\frac{-ig^{\mu\nu}}{k^2}$

Note that the propagator may have a different form under different gauge choices, but all physical results must be independent of this.

We now turn our attention to the massive vector field, described by the Proca Lagrangian:

$$\mathcal{L}_P = -\frac{1}{4} F^{\mu\nu} F_{\mu\nu} + \frac{1}{2} m^2 A^{\mu} A_{\mu}.$$

It should be noted that the mass term breaks the gauge invariance of the Lagrangian, but the standard model solves this by introducing additional terms of interaction with the Higgs boson. The corresponding equation of

motion is the Procca equation without sources: $\partial_\mu F^{\mu\nu} + m^2 A^\nu = 0$. This time, the solution accepts six different normal modes:

$$A^\mu_{k+}(x) = \epsilon^\mu_{k+} e^{-ik\cdot x},$$
$$A^\mu_{k-}(x) = \epsilon^\mu_{k-} e^{-ik\cdot x},$$
$$A^\mu_{k0}(x) = \epsilon^\mu_{k0} e^{+ik\cdot x},$$

as well as their complex conjugates, with the new polarization vector corresponding to the longitudinally polarized particle. The polarization vectors can be taken as

$$\epsilon^\mu_{k+} = \Lambda \begin{pmatrix} 0 \\ 1/\sqrt{2} \\ i/\sqrt{2} \\ 0 \end{pmatrix}, \quad \epsilon^\mu_{k-} = \Lambda \begin{pmatrix} 0 \\ 1/\sqrt{2} \\ -i/\sqrt{2} \\ 0 \end{pmatrix}, \quad \epsilon^\mu_{k0} = \Lambda \begin{pmatrix} 0 \\ 0 \\ 0 \\ 1 \end{pmatrix},$$

Where Λ is now a Lorentz transformation matrix that maps $(m, 0, 0, 0) \mapsto k$.

The three polarization vectors for an on-shell massive vector particle satisfy the projector relation [15]

$$\sum_{\lambda=+,-,0} \epsilon^{\mu *}_{k\lambda} \epsilon^\nu_{k\lambda} = -g^{\mu\nu} + \frac{k^\mu k^\nu}{k^2} \equiv -T^{\mu\nu}_k, \tag{2.2}$$

where $T^{\mu\nu}_k$ is a transversal projector in the sense that, when contracted with a four-vecor, it results in its projection to the space transversal to k. That is, $T^{\mu\nu}_k k_\mu = 0$ and $T^{\mu\nu}_k q_\mu = q_\nu$ for any q transversal to k (meaning $q_\mu k^\mu = 0$). Likewise, we define the longitudinal projector

$$L^{\mu\nu}_k \equiv \frac{k^\mu k^\nu}{k^2}$$

with the property that $L^{\mu\nu}_k k_\mu = k_\nu$ and $L^{\mu\nu}_k q_\mu = 0$ for any q transversal to k. The transversal and longitudinal projectors also satisfy the following projector identities:

$$\begin{aligned} T^{\mu\nu}_k (T_k)_{\nu\alpha} &= (T_k)^\mu_\alpha, \\ L^{\mu\nu}_k (L_k)_{\nu\alpha} &= (L_k)^\mu_\alpha, \\ T^{\mu\nu}_k (L_k)_{\nu\alpha} &= 0, \\ T^{\mu\nu}_k + L^{\mu\nu}_k &= g^{\mu\nu}. \end{aligned} \tag{2.3}$$

The propagator for the massive vector field can be written in terms of the transversal and longitudinal projectors, and the Feynman rules are:

- For each incoming particle of polarization $+/-/0$, add the polarization vector $\epsilon^{\mu}_{k(+,-,0)}$
- For each outgoing particle of polarization $+/-/0$, add the polarization vector $\epsilon^{\mu *}_{k(+,-,0)}$
- For each internal line, add the propagator $\frac{-iT^{\mu\nu}_k}{k^2-m^2} + \frac{iL^{\mu\nu}_k}{m^2}$

2.3 Gauge Symmetries

In the standard model, gauge symmetries act primarily on fermions, and bosons are introduced as a form of ensuring that this symmetry is maintained. Let us first illustrate this process by examining the Quantum Electrodynamics sector of the standard model.

Consider the Dirac Lagrangian:

$$\mathcal{L}_D = \bar{\Psi}(i\gamma^\mu \partial_\mu - m)\Psi,$$

which is invariant under the transformation $\Psi \mapsto e^{ig'\theta}\Psi$, where $g'\theta$ is a constant. This is known as a global symmetry because the transformation is applied equally at all points in space-time, as opposed to a local symmetry where the transformation can be different at each point. We could promote this to a local transformation by promoting θ to a function $\theta(x)$, but then the Lagrangian would not be invariant because the derivative would generate an additional $-g'\partial_\mu\theta(x)\bar{\Psi}\gamma^\mu\Psi$ term. Recall that the gauge invariance of the massless vector field allows it to absorb any function that is a total derivative, which can be exploited to compensate for this extra term. Indeed, we can invoke a massless field B_μ and add the term $g'B_\mu\bar{\Psi}\gamma^\mu\Psi$ to the Lagrangian, asking that the vector field transforms simultaneously with Ψ as $B_\mu \mapsto B_\mu + \partial_\mu\theta(x)$. From now on we refer to this transformation, which acts locally on the vector field and the Dirac field simultaneously, as the gauge transformation. When the new $g'B_\mu\bar{\Psi}\gamma^\mu\Psi$ term undergoes the gauge transformation, it gains an additional $+g'\partial_\mu\theta(x)\bar{\Psi}\gamma^\mu\Psi$ term, which precisely cancels the previous extra term. Notice that adding the $g'B_\mu\bar{\Psi}\gamma^\mu\Psi$ term to the Lagrangian corresponds to substituting the partial derivative by a *covariant derivative*:

$$\partial_\mu \mapsto D_\mu \equiv \partial_\mu - ig'B_\mu,$$

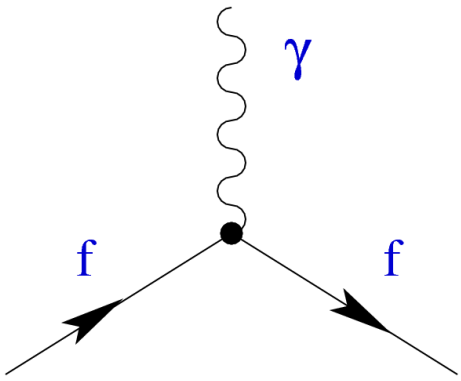

Figure 2.1: QED vertex coupling two fermion lines (f) to a photon line (γ).

so the full gauge-invariant Lagrangian (including the free Maxwell Lagrangian) can be written as

$$\mathcal{L}_{QED} = \bar{\Psi}(i\gamma^\mu D_\mu - m)\Psi - \frac{1}{4}F^{\mu\nu}F_{\mu\nu}.$$

In order to preserve the gauge symmetry, we had to add a new term which couples two fermion lines to a vector line. If B_μ were the photon field, this would be what is known as the QED vertex (Fig. 2.1), and because g' is the coupling constant that modulates it, it would be clear that it represents the electric charge (denoted by e) of the particle. This is not strictly the case because the photon field is a mixture of the B_μ field and the W^3_μ field that we will soon discuss. If we ignore this subtlety for now, however, we arrive to the Feynman rule for the QED interaction:

- For each QED vertex, add $-ie\gamma^\mu$

The gauge symmetry that we have worked with so far is known as a $U(1)$ symmetry because it acts on a single fermion field by multiplying it by a phase. However, we can also have other symmetry groups that act on multiple fields by mixing them. For instance, consider the group $SU(2)$ of 2×2 unitary matrices with determinant 1, which can act on a 2x1 column of left-handed spinors Ψ_L and χ_L:

$$\begin{pmatrix}\Psi_L \\ \chi_L\end{pmatrix} \mapsto G \begin{pmatrix}\Psi_L \\ \chi_L\end{pmatrix}, \quad G \in SU(2).$$

By definition, the transformation acts only on the left-handed components while doing nothing to the right-handed components. Because Ψ_L and χ_L

are affected by the $SU(2)$ tranformation jointly, they are said to form an $SU(2)$ *doublet*, whereas Ψ_R and χ_R are $SU(2)$ *singlets*. We can write the free Lagrangian of both particles as

$$\begin{aligned}\mathcal{L} =&\bar{V}_L\gamma^\mu\partial_\mu V_L + \bar{\Psi}_R\gamma^\mu\partial_\mu\Psi_R + \bar{\chi}_R\gamma^\mu\partial_\mu\chi_R \\ &- m_\Psi\left(\bar{\Psi}_L\Psi_R + \bar{\Psi}_R\Psi_L\right) - m_\chi\left(\bar{\chi}_L\chi_R + \bar{\chi}_R\chi_L\right),\end{aligned}$$

where

$$V_L = \begin{pmatrix}\Psi_L \\ \chi_L\end{pmatrix} \qquad \text{and} \qquad \bar{V}_L = \begin{pmatrix}\bar{\Psi}_L & \bar{\chi}_L\end{pmatrix}.$$

Any transformation $G \in SU(2)$ can be written as

$$G:\ V_L \mapsto e^{i\theta_i\sigma_i}V_L$$

for some choice of constants θ_i, where we sum over $i = 1, 2, 3$ and σ_i are the pauli matrices, which are the generators of $SU(2)$. As before, the Lagrangian is invariant under any such global transformation, but not if we consider local transformations by taking $\theta_i(x)$ as functions. This time we need three vector fields, one for each generator, in order to make the symmetry local. We denote these fields by $\vec{W}_\mu = (W^1_\mu, W^2_\mu, W^3_\mu)$ and define the 2×2 matrix field

$$W_\mu \equiv \frac{i}{2}\vec{W}_\mu \cdot \vec{\sigma}.$$

To extend $SU(2)$ to a gauge symmetry we ask that W^μ transforms as

$$W_\mu \mapsto G(x)\left[W_\mu(x)\frac{1}{g}\partial_\mu\right]G^\dagger(x),$$

where g is a new coupling constant, and replace the partial derivative with a new covariant derivative defined as

$$D_\mu \equiv \partial_\mu\mathbb{I} + gW_\mu(x),$$

where $\mathbb{I}$ is the 2×2 unitary matrix which will be omitted from now on.

This is equivalent to adding the interaction term

$$\begin{aligned}ig\bar{V}_L\gamma^\mu W_\mu V_L = -\frac{g}{\sqrt{2}}\Bigg[&W^+_\mu\bar{\Psi}_L\gamma^\mu\chi_L + W^-_\mu\bar{\chi}_L\gamma^\mu\Psi_L \\ &+ \frac{W^3_\mu}{\sqrt{2}}\left(\bar{\Psi}_L\gamma^\mu\Psi_L - \bar{\chi}_L\gamma^\mu\chi_L\right)\Bigg],\end{aligned}$$

where we have introduced the fields

$$W_\mu^\pm \equiv \frac{1}{\sqrt{2}}\left(W_\mu^1 \mp iW_\mu^2\right)$$

which represent the charged W bosons that are observable according to the standard model.

In order to replicate the electroweak interaction of the standard model in the leptonic sector, let us now consider this SU(2) symmetry joint to a U(1) symmetry that acts with coupling constant g' on χ_R, 0 on Ψ_R, and $g'/2$ on Ψ_L, χ_L. In this case, the sum of all interaction terms is

$$\begin{aligned}\bar{V}_L\gamma^\mu\left(\frac{g'}{2}B_\mu - gW_\mu^3\right)V_L + g'\bar{\chi}_R\gamma^\mu B_\mu\chi_R = \\ -\frac{g}{\sqrt{2}}\left[W_\mu^+\bar{\Psi}_L\gamma^\mu\chi_L + W_\mu^-\bar{\chi}_L\gamma^\mu\Psi_L\right] - eA_\mu\bar{\chi}\gamma^\mu\chi \\ - g_1Z_\mu\bar{\Psi}_L\gamma^\mu\Psi_L - g_2Z_\mu\bar{\chi}_L\gamma^\mu\chi_L - g_3Z_\mu(\bar{\Psi}_R\gamma^\mu\Psi_R + \bar{\chi}_R\gamma^\mu\chi_R),\end{aligned}$$

where we have defined the photon and Z-boson fields

$$A_\mu \equiv \frac{g'W_\mu^3 + gB_\mu}{\sqrt{g^2+g'^2}} \qquad \text{and} \qquad Z_\mu \equiv \frac{gW_\mu^3 - g'B_\mu}{\sqrt{g^2+g'^2}},$$

which correspond to the observable particles of the standard model, and the new coupling constants are defined as

$$e \equiv \frac{gg'}{\sqrt{g^2+g'^2}}, \qquad g_1 \equiv \frac{\sqrt{g^2+g'^2}}{2}, \qquad g_2 \equiv \frac{g'^2-g^2}{2\sqrt{g^2+g'^2}}, \qquad g_3 \equiv \frac{g'^2}{\sqrt{g^2+g'^2}}.$$

This change of basis is done so that the photon field A_μ couples to left- and right-handed components indistinctly, and also such that A_μ and Z_μ are the mass eigenstates which originate from the interaction with the Higgs boson (discussed in the following section).

Notice that only the χ field is coupled to the photon and since e is the constant that modulates this interaction, it is clear that it represents the electric charge. This term represents the electromagnetic interaction and is the same as the QED vertex we had considered before, except the charge now has its proper value and the coupling is with the actual photon field. The fact that only χ is charged suggests that our doublet consists of a charged lepton χ and a neutrino Ψ, and is a consequence of our choice of coupling constants

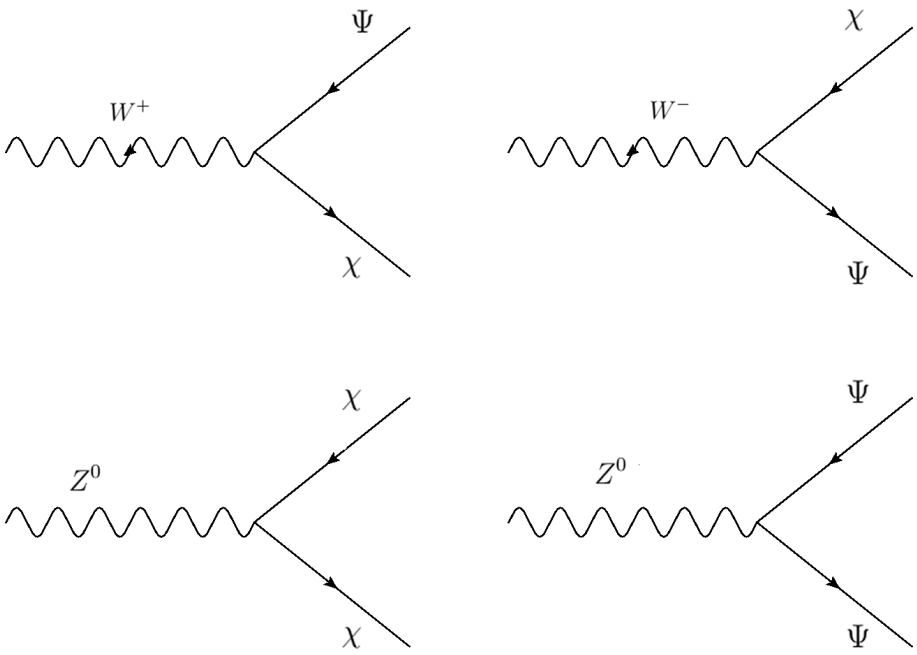

Figure 2.2: Charged current (top) and neutral current (bottom) interactions for any pair of fermions Ψ_L, χ_L that form an SU(2) doublet.

for the U(1) symmetry (a choice of $g'/6$ for the left-handed spinors, $2g'/3$ for Ψ_R and $-g'/3$ for χ_R would have resulted in Ψ and χ having electric charges $2e/3$ and $-e/3$, respectively, which is the familiar case of the quark doublet). The two terms in the bracket account for the *charged current interaction*, mediated by the $W^{\pm}$ bosons, while the last three terms represent *neutral current interactions*, mediated by the Z boson. These interactions are shown in Fig. 2.2.

By noting that we can rewrite

$$\bar{\Psi}_L \gamma^\mu \chi_L = \frac{1}{2} \bar{\Psi} \gamma^\mu \left(1 - \gamma_5\right) \chi \qquad \text{and} \qquad \bar{\chi}_L \gamma^\mu \Psi_L = \frac{1}{2} \bar{\chi} \gamma^\mu \left(1 - \gamma_5\right) \Psi,$$

we arrive at the Feynman rule for the charged current interaction:

- For each charged current vertex, add the coupling $i\frac{g}{2\sqrt{2}}\gamma^\mu(1-\gamma_5)$

and a similar rule can be derived for the neutral current interaction. Because the term $\gamma^\mu \left(1 - \gamma_5\right)$ in-between spinors has the structure of a vector minus an axial vector, this is often referred to as a *V-A coupling*.

2.4 The Standard Model

The standard model of particle physics includes twelve kinds of fermions divided into six *quarks* and six *leptons*, together with twelve kinds of gauge bosons and one Higgs boson. Fig. 2.3 shows a graphical summary of all the particles considered in the standard model.

The *up*, *charm* and *top* quarks have electric charge +2/3 and are denoted by the letters u, c, t or u_1, u_2, u_3 when refered to as *type-up* quarks. Meanwhile, the *down*, *strange* and *bottom* quarks have electric charge -1/3 and are denoted by the letters d, s, b or d_1, d_2, d_3 when refereed to as *type-down* quarks. The left-handed component of each type-up quark forms an SU(2) doublet with the left-handed component of the corresponding type-down quark, denoted by

$$Q_i = \begin{pmatrix} u_{iL} \\ d_{iL} \end{pmatrix}, \quad i = 1, 2, 3$$

while the right-handed components form SU(2) singlets.

On the lepton side, there are three *flavors* that we call *electronic*, *muonic* and *tauonic*, and each flavor has a charged lepton (denoted e, μ, τ) of electric charge -1 and a corresponding neutrino (denoted ν_e, ν_μ, ν_τ) of electric charge 0. Each left-handed charged lepton forms an SU(2) doublet with the corresponding left-handed neutrino, denoted by

$$L_l = \begin{pmatrix} \nu_{lL} \\ l_L \end{pmatrix}, \quad l = e, \mu, \tau$$

while the right-handed components form SU(2) singlets.

Thus, the Lagrangian that includes both the U(1) and SU(2) gauge symmetries, with the U(1) couplings described in the last section, can be written

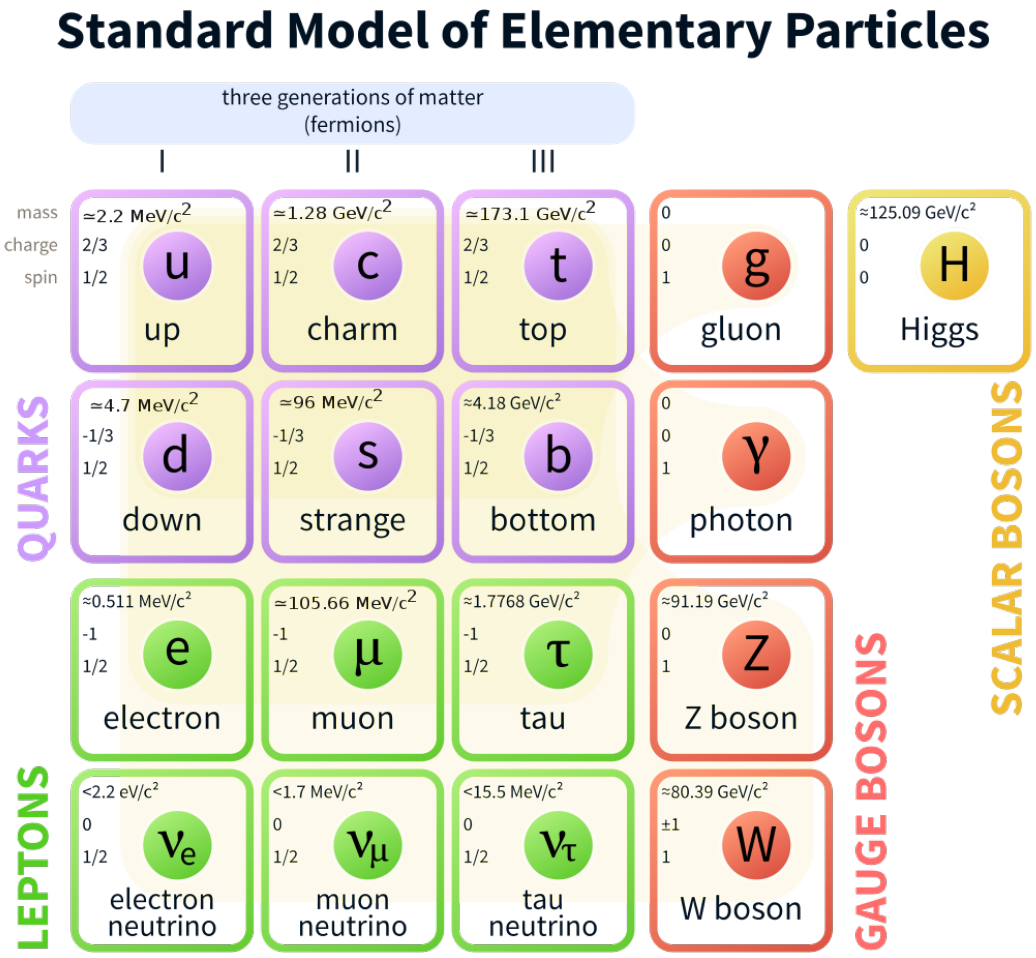

Figure 2.3: Particles of the standard model, divided into quarks (top left), leptons (bottom left) and gauge bosons (right).

(excluding the kinetic boson terms and the masses) as

$$\mathcal{L} = \sum_{i=1,2,3} \Bigg[\bar{Q}_{iL}\gamma^\mu \left(\partial_\mu - i\frac{g'}{6}B_\mu + gW_\mu\right) Q_{iL}$$

$$+ \bar{u}_{iR}\gamma^\mu \left(\partial_\mu + i\frac{2g'}{3}B_\mu\right) u_{iR} + \bar{d}_{iR}\gamma^\mu \left(\partial_\mu - i\frac{g'}{3}B_\mu\right) d_{iR} \Bigg]$$

$$+ \sum_{l=e,\mu,\tau} \Bigg[\bar{L}_l\gamma^\mu \left(\partial_\mu - i\frac{g'}{2}B_\mu + gW_\mu\right) L_l \tag{2.4}$$

$$+ \bar{l}_R\gamma^\mu \left(\partial_\mu - ig'B_\mu\right) l_R + \bar{\nu}_{lR}\gamma^\mu \left(\partial_\mu\right) \nu_{lR} \Bigg] \tag{2.5}$$

The concept of lepton flavor universality in the standard model refers to the fact that the coupling constants to the B and W fields are assumed to remained unchanged when switching flavors (although of course they are different for the charged leptons than for the neutrinos), and studying processes involving the charged current interaction allows us to test this hypothesis, at least for the g coupling.

The standard model considers another scalar particle called the Higgs boson, which arises as two complex fields that form an SU(2) doublet and couple to the $W^\pm$ and Z^0 bosons, as well as all quarks and charged leptons, allowing them to have a mass term without breaking the gauge symmetry upon experiencing a *spontaneous symmetry breaking*, which also results in several couplings among bosons in what is known as the *Higgs mechanism*.

The weak interaction also exhibits quark flavor mixing. This is so because the quark fields that couple to the gauge fields (called the flavor eigenstates) need not be in the same basis as the ones that appear in the mass terms (called the mass eigenstates), which are the ones that interact with the Higgs boson. In particular, we could replace the quark fields in the first line of (2.5) by fields u'_{iL}, d'_{iL} in a different flavor basis, related to the original fields by 3×3 unitary matrices $U^{(u)}, U^{(d)}$ as follows:

$$\begin{pmatrix} u_L \\ c_L \\ t_L \end{pmatrix} = U^{(u)} \begin{pmatrix} u'_L \\ c'_L \\ t'_L \end{pmatrix} \qquad \text{and} \qquad \begin{pmatrix} d_L \\ s_L \\ b_L \end{pmatrix} = U^{(d)} \begin{pmatrix} d'_L \\ s'_L \\ b'_L \end{pmatrix},$$

which also implies

$$\begin{pmatrix} \bar{u}_L & \bar{c}_L & \bar{t}_L \end{pmatrix} = \begin{pmatrix} \bar{u}'_L & \bar{c}'_L & \bar{t}'_L \end{pmatrix} U^{(u)\dagger}$$

and

$$\begin{pmatrix} d_L & s_L & b_L \end{pmatrix} = \begin{pmatrix} \bar{d}'_L & \bar{s}'_L & \bar{b}'_L \end{pmatrix} U^{(d)\dagger}.$$

Notice that we could have done the same for the right-handed fields, but because the matrices commute with the ∂_μ and B_μ terms, they would cancel because of the unitarity. In fact, this is true for all currents that match a spinor with its conjugate spinor, and the only difference arises with the charged currents that match type-up quarks to type-down quarks. The form of these currents in the new basis will now be

$$\begin{aligned}
L_{c.c.} &= -\frac{g}{\sqrt{2}} \sum_{i=1,2,3} \left[W^+_\mu \bar{u}_i \gamma^\mu d_i + W^-_\mu \bar{d}_i \gamma^\mu u_i \right] \\
&= -\frac{g}{\sqrt{2}} \left[W^+_\mu \begin{pmatrix} \bar{u}_L & \bar{c}_L & \bar{t}_L \end{pmatrix} \gamma^\mu \begin{pmatrix} d_L \\ s_L \\ b_L \end{pmatrix} + W^-_\mu \begin{pmatrix} \bar{d}_L & \bar{s}_L & \bar{b}_L \end{pmatrix} \gamma^\mu \begin{pmatrix} u_L \\ c_L \\ t_L \end{pmatrix} \right] \\
&= -\frac{g}{\sqrt{2}} \left[W^+_\mu \begin{pmatrix} \bar{u}'_L & \bar{c}'_L & \bar{t}'_L \end{pmatrix} \gamma^\mu U^{(u)\dagger} U^{(d)} \begin{pmatrix} d'_L \\ s'_L \\ b'_L \end{pmatrix} \right. \\
&\qquad \left. + W^-_\mu \begin{pmatrix} \bar{d}'_L & \bar{s}'_L & \bar{b}'_L \end{pmatrix} \gamma^\mu U^{(d)\dagger} U^{(u)} \begin{pmatrix} u'_L \\ c'_L \\ t'_L \end{pmatrix} \right] \\
&= -\frac{g}{\sqrt{2}} \sum_{i,j=1,2,3} \left[W^+_\mu V_{u_i d_j} \bar{u}'_i \gamma^\mu d'_j + W^-_\mu V^*_{u_i d_j} \bar{d}'_j \gamma^\mu u'_i \right],
\end{aligned}$$

where we have defined the Cabibbo–Kobayashi–Maskawa matrix $V \equiv U^{(u)\dagger} U^{(d)}$ with components $V_{u_i d_j} = (V)_{ij}$. Thus, in the standard model we obtain charged currents connecting quarks of different flavors at the price of introducing the CKM matrix element in the Feynman rules for each vertex. In practice, the measurements of the CKM matrix have found it to be close to the identity, so that charged currents connect mostly quarks of the same flavor and flavor mixing is minimal. This exact same procedure can be repeated for the left-handed leptons, but the distinction between flavor and mass eigenstate is meaningless until we consider neutrino mass terms. If we assume that neutrinos are Dirac fermions (that is, that they have mass terms of the same form as the other Dirac fields), the equivalent of the CKM matrix that we obtain is known as the Pontecorvo–Maki–Nakagawa–Sakata matrix. Unlike the CKM matrix, the PMNS matrix has been found to deviate strongly from the identity. We will not consider neutrino masses, so that

the flavor eigenstates can be taken to be mass eigenstates and flavor mixing does not occur in the leptonic sector.

It should be noted that each type of quark actually has three spinor fields, which we refer to as its *color components*. The standard model considers one more gauge symmetry, which is given by the group $SU(3)$ and acts on the color components of each quark by mixing them. Thus, we say that the full gauge symmetry of the standard model is a $U(1) \times SU(2) \times SU(3)$ symmetry. In order to conserve the $SU(3)$ symmetry locally, the standard model also incorporates 8 new bosons (which is the number of SU(3) generators) called *gluons*, in addition to the four already needed for the $U(1)$ and $SU(2)$ symmetries. The interactions that arise, called *strong interactions*, form the basis of *Quantum Chromodynamics*. We will not delve too much into QCD, but we do note that, unlike the other theories, it exhibits a phenomenon known as *asymptotic freedom* which means that the couplings become asymptotically null at large energies. Conversely, the couplings also become increasingly strong at low energies (or large distances), which leads to the phenomenon of *confinement*, meaning that quarks can never exist as free particles but are always found in color-neutral multi-quark systems known as *hadrons*. On a practical level, this also complicates the calculation of QCD processes because higher order diagrams cannot be simply neglected, so processes involving quarks often require experimental measurement of form factors rather than direct theoretical calculations.

2.5 The Quark Model

As we have previously mentioned, quarks cannot exist as free particles and are always confined to color-neutral multi-quark states called hadrons. The most simple types of hadrons are one quark and one antiquark of the same color, which form systems known as *mesons*, and three quarks of complementing colors which form systems known as *baryons*. Because the running strong coupling cannot be considered a perturbation, systems with more elaborated structures are no less likely to appear. Therefore, the real mesons and baryons that we observe are actually a complex conglomerate of quarks and gluons with net zero couplings to other gauge fields, plus an excess two or three quarks (respectively). The description of hadrons in terms of these *valence quarks* is known as the quark model, and it should come as no surprise that the mass of the hadrons is usually much larger than the sum of its valence

quarks' masses. In this section we consider the quark model for mesons only, as they are the ones that play an important role in our work.

Let us first consider only the u and d quarks. Since they (or their left-handed components at least) form a doublet that transforms under the $SU(2)$ group, which is the same group used for the spin-1/2 representation in quantum physics, we can form an analogy where a quark is a particle of total *isospin* 1/2 and the u quark represents a state of isospin projection $T_3 = +1/2$, while the d quark represents the isospin projection $T_3 = -1/2$. The consideration of the u and d quarks as different states of the same particle is known as isospin symmetry, an is only an approximation once we consider their slight difference in mass. When we add two quarks together to form a meson, we can either get a system of total isospin 1 or 0. The states of total isospin 1 are known as pions, with the projections $T_3 = -1, 0, 1$ denoted π^-, π^0, π^+ respectively, while the state of total isospin 0 is denoted η^0. In complete analogy to spin addition, these states are given by

$$\begin{aligned} |\pi^+\rangle &= |uu\rangle \\ |\pi^0\rangle &= \frac{1}{\sqrt{2}}\left(|ud\rangle + |du\rangle\right) \\ |\pi^-\rangle &= |dd\rangle \\ |\eta_0\rangle &= \frac{1}{\sqrt{2}}\left(|ud\rangle - |du\rangle\right). \end{aligned}$$

Let us now consider the s quark, to which we will not assign any isospin structure (it is a particle of isospin 0). In fact, the concept of isospin is not useful for any of the other quark families, because the mass differences are much larger and the symmetry is vastly broken. Instead, we distinguish hadrons containing s quarks by a property called *strangeness*. The s quark is said to have strangeness -1, and can couple with an anti-u or d quark to form the kaon states K^- and K^0, respectively. Meanwhile, the anti-s quark is said to have strangeness +1 an can couple to an u or d quark to form the K^+ and $\bar{K}^0$. We can form yet another state, called the η_s, by coupling an $s\bar{s}$ pair. Note that both η_0 and η_s are states of zero total isospin and zero strangeness, so we could get eigenstates from any mixture of them. The actual energy eigenstates, called the η and η', are indeed mixtures of η_0 and η_s, which are due to the flavor mixing of the weak interaction.

The u, d and s quarks that we have considered so far are usually considered light quarks, and they form the eight most common types of mesons,

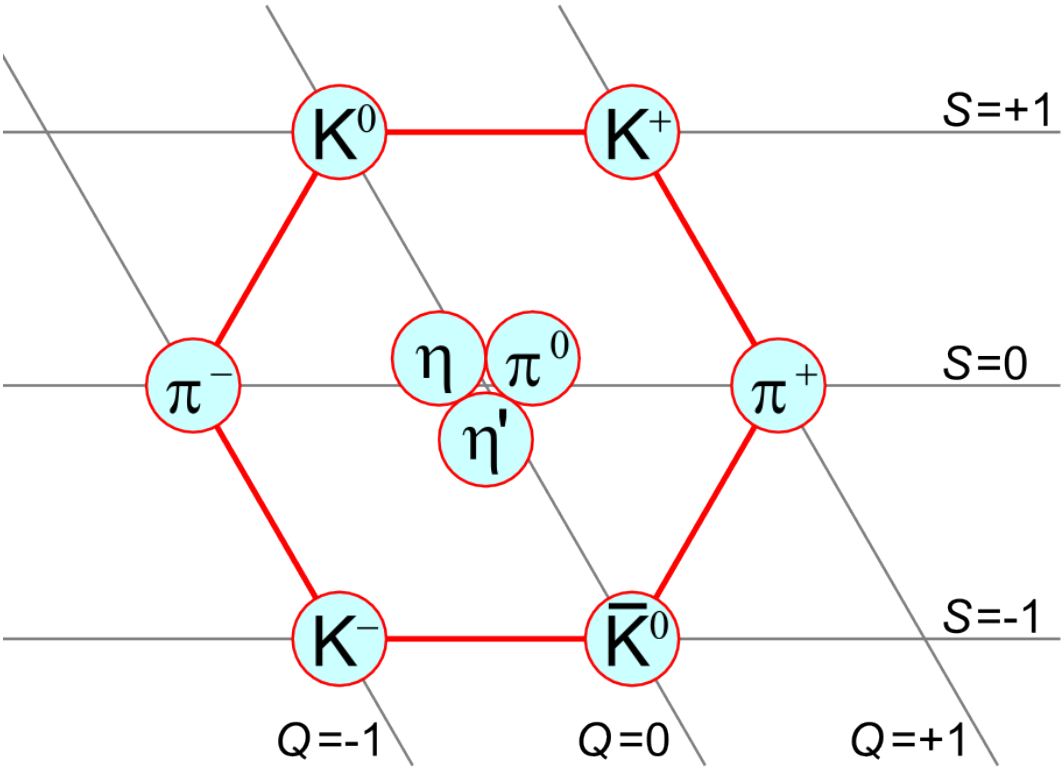

Figure 2.4: Mesons formed by the u, d and s quarks form the eightfold way, where horizontal lines represent constant strangeness and diagonal lines represent constant electric charge. The η' state has been added to this diagram, bringing the total number of mesons up to nine.

often summarized graphically in an arrangement called the *Eightfold Way* [18], plus the additional singlet state η' as shown in Fig. 2.4. Mesons that include a c or b quark are known as heavy mesons. The t quark has never been observed to form hadrons, since its mass is so large that it usually decays before forming any bound states. The c quark can couple to an anti-u, d or s quark, forming the D^0, D^+ and D_s^+ mesons, respectively, while the anti-c quark can couple to an u, d or s quark to form the $\bar{D}^0$, D^- and D_s^- mesons. Likewise, the b quark couples to anti-u, d, s and c quarks to form the B^-, B^0, B_s^0 and B_c^- mesons, and the anti-b couples to u, d, s and c to form the B^+, $\bar{B}^0$, $\bar{B}_s^0$ and B_c^+.

Because each quark is a spin-1/2 particle, each meson system can be in either a spin-0 or a spin-1 configuration. Note that quarks and antiquarks must always have opposite parities, so all ground-state mesons must have parity -1. This means that ground-state spin-0 mesons are pseudoscalars, while ground-state spin-1 mesons are vectors. When a meson is not in its ground state, it may have an orbital angular momentum (denoted L), and the parity is switched for each unit of L, so the parity is given by $P = (-1)^{1+L}$. When considering ground-state mesons, the pseudoscalar configurations are denoted by the letters we have been using so far, while the vector configurations are denoted with a star (*e.j.* D^{*-}). A special exception is considered for the vector configurations of the pions, the η and the η', which are denoted by the letters ρ, ω and φ (without a star), respectively.

The mesons that are relevant for our work are the $B^{0,\pm}$, $D^{*\mp,0}$, $D^{\mp,0}$ and $\pi^{\pm,0}$. The properties of these mesons are listed in Table 2.1. As mentioned in the introduction, the $B \to l\nu D^*$ decay arises naturally from a $b \to c$ quark transition which has a large mass difference that enables tau production, with a spectator u or d quark. One could also consider an s spectator quark, leading to the analogous process

$$B_s \to l\nu D_s^*$$

which has been studied before [19, 20], but its theoretical description is more complicated due to the fact that the s quark mass is not as small as that of the u and d when compared to that of the c, which makes the heavy quark approximation (discussed in section 3.4) less useful. There is also a lack of experimental data to compare with for this case and we do not delve into it because, moreover, the D_s^* decay is dominated by the $D_s\gamma$ mode even for the charged case, so longitudinal corrections are not applicable.

2.6 Decay Processes

In this section we consider the problem of integrating a squared amplitude to obtain the cross section of a process. In particular, we limit ourselves to considering decay processes of one particle into three or four products. Our discussion and the parametrization that we use closely follows the one found in [21]. Once the squared amplitude for a process into N products is calculated, it must be integrated over the momenta of the outgoing particles

Table 2.1: Properties of the mesons present in the $B \to l\nu\pi D$ decay. The $I(J^P)$ notation represents the quantum numbers for $isospin(total\ spin^{parity})$

Particle Symbol	Valence Quarks	$I(J^P)$	Mass (MeV)
$B^{\pm}/B^0$	$u\bar{b}/d\bar{b}$	$\frac{1}{2}(0^-)$	5279
$D^{*\pm}/D^{*0}$	$d\bar{c}/u\bar{c}$	$\frac{1}{2}(1^-)$	2010/2007
$D^{\pm}/D^0$	$d\bar{c}/u\bar{c}$	$\frac{1}{2}(0^-)$	1870/1865
$\pi^{\pm}/\pi^0$	$u\bar{d}/\frac{1}{\sqrt{2}}(u\bar{u}+d\bar{d})$	$1(0^-)$	140/135

in order to get the decay width, while enforcing each outgoing particle to be on shell and requiring momentum conservation as follows:

$$\Gamma = \int \frac{|M|^2}{2E_0}(2\pi)^4\delta^4\left(p_0 - \sum_{i=1}^{N} p_i\right)\prod_{i=1}^{N}\left(\frac{d^4p_1}{(2\pi)^3}\delta(p_1^2 - m_1^2)\right),$$

where p_i, m_i are the momenta of the outgoing particles and E_0 is the energy of the initial particle.

Let us first consider a decay into three bodies using for convenience the notation of the $B \to l\nu D^*$ decay with the momenta and masses of the respective particles given by $p_B, p_l, p_\nu, p_{D^*}, m_B, m_l, m_\nu, m_{D^*}$. We also work in the rest frame of the system, so that $E_0 = m_B$. By enforcing momentum conservation, all scalar products can be written in terms of the two variables:

$$s \equiv (p_B - p_{D^*})^2 = (p_l + p_\nu)^2 \qquad \text{and} \qquad u \equiv (p_B - p_\nu)^2 = (p_l + p_{D^*})^2,$$

and the three-body decay width can be rewritten as

$$\Gamma_3 = -\int_{s_-}^{s_+}\int_{u_-}^{u_+} \frac{|M(u,s)|^2}{2m_B(2\pi)^5}\, du\, ds,$$

where we have used $|M(u,s)|^2$ to refer to the square amplitude in terms of only u and s once momentum conservation has been enforced, and the limits of integration are

$$s_- = (m_l + m_\nu)^2, \qquad s_+ = (m_B - m_{D^*})^2,$$

$$u_\pm = m_B^2 + m_\nu^2 - \frac{(s + m_\nu^2 - m_l^2)(m_B^2 + s - m_{D^*}^2)}{2s} \pm \frac{\lambda^{1/2}(s, m_\nu^2, m_l^2)\lambda^{1/2}(m_B^2, s, m_{D^*}^2)}{2s},$$

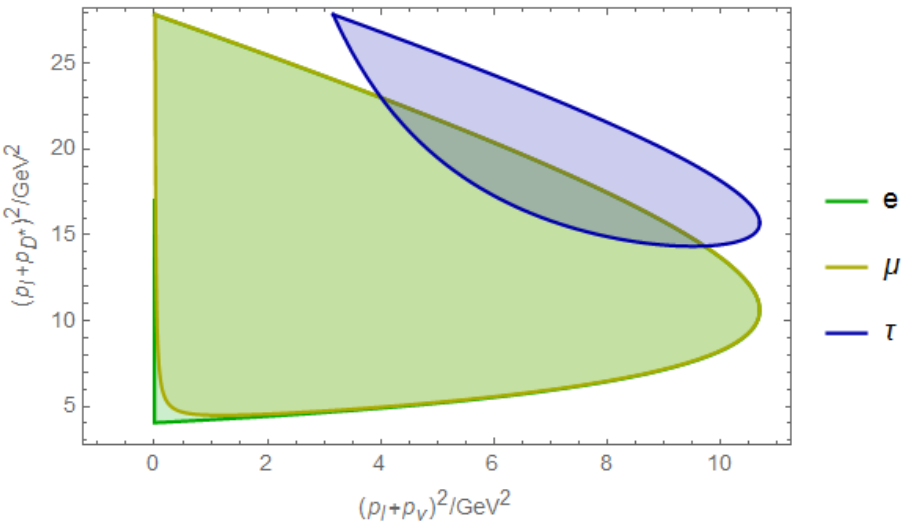

Figure 2.5: Dalitz plots representing the phase space for the $B \to l\nu D^*$ decay for each lepton flavor.

with

$$\lambda(x, y, z) \equiv x^2 + y^2 + z^2 - 2xy - 2xz - 2yz. \tag{2.6}$$

These limits define a phase space region known as the *Dalitz region*, which is plotted in Fig. 2.5 for the particles in question, for each of the lepton flavors. Notice that for the electron and the muon the phase space is almost identical, so we can usually talk about the "light flavor" case indistinctly. This is to be expected, since both masses are negligible compared to the energy scale of the process (given by the mass of the B), but the same is not true for the tau.

Once we consider the full $B \to l\nu\pi D$ process, we need the four-body phase space. We again use the usual notation for the momenta and masses of the B, l, ν, π, D, and also use $p_{D^*} \equiv p_D + p_\pi$ while noting that this is no longer an on-shell momentum. This time we can write all scalar products in terms of five variables:

$$s_1 \equiv (p_B - p_l)^2 = (p_\nu + p_\pi + p_D)^2, \qquad s_2 \equiv (p_B - p_l - p_\nu) = p_{D^*}^2,$$

$$u_1 \equiv (p_B - p_\nu)^2 = (p_l + p_\pi + p_D)^2, \qquad u_2 \equiv (p_B - p_\pi)^2 = (p_l + p_\nu + p_D)^2,$$

$$\text{and} \qquad t \equiv (p_B - p_\nu - p_\pi)^2 = (p_l + p_D)^2,$$

and the four-body decay width can be rewritten as

$$\Gamma_4 = \int \frac{|M|^2 ds_2 ds_1}{2m_B(2\pi)^8} \frac{du_1 du_2}{\lambda^{1/2}(m_B^2, s_2, s_2')\lambda^{1/2}(m_B^2, m_\pi^2, u_2)} \times \frac{dt}{\lambda^{1/2}(m_B^2, u_1, m_l^2)[(1-\xi^2)(1-\eta^2)(1-\zeta^2)]^{1/2}},$$

where

$$s_2' \equiv s_2 - s_1 - u_1 + m_B^2 + m_l^2 + m_\nu^2$$

and the functions ξ, η, ζ are defined as follows:

$$\xi \equiv \frac{(m_B^2 + s_2' - s_2)(m_B^2 + m_l^2 - u_1) - 2m_B^2 s_2'}{\lambda^{1/2}(m_B^2, s_2, s_2')\lambda^{1/2}(m_B^2, m_\pi^2, u_2)},$$

$$\eta \equiv \frac{2m_B^2(s_2 + m_\pi^2 - m_D^2) - (m_B^2 + m_\pi^2 - u_2)(m_B^2 + s_2 - s_2')}{\lambda^{1/2}(m_B^2, s_2, s_2')\lambda^{1/2}(m_B^2, m_\pi^2, u_2)},$$

and

$$\zeta \equiv (\omega - \xi\eta)\sqrt{(1-\xi^2)(1-\eta^2)}$$

with

$$\omega \equiv \frac{2m_B^2(u_1 + m_\pi^2 - t) - (m_B^2 + m_\pi^2 - u_2)(m_B^2 + u_1 - m_l^2)}{\lambda^{1/2}(m_B^2, u_1, m_l^2)\lambda^{1/2}(m_B^2, m_\pi^2, u_2)}.$$

The limits for the integration are:

$$s_2^- = (m_\pi + m_D)^2, \qquad s_2^+ = (m_B - m_l - m_\nu)^2,$$

$$s_1^- = (\sqrt{s_2} + m_\nu)^2, \qquad s_1^+ = (m_B - m_l)^2,$$

$$u_1^\pm = m_B + m_\nu^2 - \frac{(s_1 + m_\nu^2 - s_2)(m_B + s_1 - m_\nu^2)}{2s_1} \pm \frac{\lambda^{1/2}(s_1, m_\nu^2, s_2)\lambda^{1/2}(m_B^2, s_1, m_\nu^2)}{2s_1},$$

$$u_2^\pm = m_B + m_\pi^2 - \frac{(s_2 + m_\pi^2 - m_D^2)(m_B - s_2 - s_2')}{2s_2} \pm \frac{\lambda^{1/2}(s_2, m_\pi^2, m_D^2)\lambda^{1/2}(m_B, s_2, s_2')}{2s_2},$$

and

$$t^{\pm} = u_1 + m_\pi^2 - \frac{(m_B^2 + m_\pi^2 - u_2)(m_B^2 + u_1 - m_l^2)}{2m_B^2} + \frac{\lambda^{1/2}(m_B^2, m_\pi^2, u_2)\lambda^{1/2}(m_B^2, u_1, m_l^2)}{2m_B^2}\left(-\xi\eta \pm \sqrt{(1-\xi^2)(1-\eta^2)}\right).$$

Notice that the invariant mass of the D^*, which may be off-shell in general, has been isolated in the variable $s_2 \equiv p_{D^*}^2$. We have left this variable as the outermost integration variable, so that the limits $s_2^{\pm}$ do not depend on any other variables. Therefore, taking the D^* to be on-shell corresponds to simply ignoring the s_2 integral and setting $s_2 = m_{D^*}^2$ (we will discuss how the on-shell limit arises in the following chapter).

Chapter 3

$B \to l\nu D^*$ and $B \to l\nu\pi D$ Decay Processes

In this section we develop all the process-specific theory needed to study the $B \to l\nu\pi D$ decay process. We begin in section 3.1 by comparing and contrasting this process with the shortened $B \to l\nu D^*$ version, and point out exactly how the so-called longitudinal corrections arise. We also write down the general form of the amplitude for the process, and then dedicate the next three sections to describing each of its ingredients in more depth: In section 3.2 we discuss the vector propagators of the W and D^* and tackle the issue of renormalization for the D^*; in section 3.3 we describe the leptonic charged current; and in section 3.4 we study the strong-interaction vertex connecting the $B - D^* - W$ and detail the parametrization that we use for our numerical calculations.

3.1 Decay Amplitudes for the B $\to$ lνD* and B $\to$ l$\nu\pi$D Decays

We begin by writing out the general forms of the amplitudes for the $B \to l\nu D^*$ and $B \to l\nu\pi D$ decay processes, describing how part of the later can be reduced into the former but also pointing out the new terms that give place to the longitudinal corrections we have alluded to.

As we have mentioned before, the decay that is observable to the experiments is closer to the four-body process shown in Fig. 3.1, but the results

are usually compared with the theoretical calculation [2] for the ratio

$$R_{D^*} \equiv \frac{BR(B \to \tau \nu_\tau D^*)}{BR(B \to l \nu_l D^*)}, \quad l = e, \mu$$

which considers only the three-body decay. We argue that it is more appropriate to compare with the ratio obtained from the four body decay, which we call

$$R_{D\pi} \equiv \frac{BR(B \to \tau \nu_\tau \pi D)}{BR(B \to l \nu_l \pi D)}, \quad l = e, \mu.$$

It is often thought that these processes can be made equivalent by considering the $B \to l\nu D^*$ decay and the $D^* \to D\pi$ decay as separate, subsequent processes, by "cutting" the diagram as shown in Fig. 3.1. When doing this, the D^* is considered first as an outgoing particle and then as an incoming particle, so it is always on shell. Specifically, we write

$$M = \sum (M_3^\mu \epsilon_\mu^*)(\epsilon_\nu M_2^\nu),$$

where M_3 is the $B \to l\nu D^*$ amplitude with the D^* polarization vector ϵ_μ^* factored out and M_2^ν is the $D^* \to D\pi$ amplitude with the D^* polarization ϵ_ν factored out, and the sum is over polarizations. At this point, it appears as though the amplitude factors into independent pieces. Moreover, the amplitude $\epsilon_\nu M_2^\nu$, which represents the $D^* \to D\pi$ decay, has no dependence on the lepton, which is produced in the other factor of the amplitude, so one might assume that this contribution cancels out in the ratio, which would justify working only with the $B \to l\nu D^*$ decay. This is not strictly the case, however, because in order for the D^* to connect the two processes the two polarization vectors must be the same and so the two factors are not independent. More specifically, we can use the polarization sum rule described in (2.2) to write

$$M = M_3^\mu \left(-g_{\mu\nu} + \frac{(p_{D^*})_\mu (p_{D^*})_\nu}{m_{D^*}^2} \right) M_2^\nu, \tag{3.1}$$

where it is clear that the factorization has been lost. Moreover, although the amplitude M_2^ν is independent of the lepton, the phase space region where it is to be integrated is not. We have already shown in Fig. 2.5 that the Dalitz region for the τ is drastically different than the region for the light leptons, so even if the part being added is lepton-independent there is no reason to think that its contribution cancels out in the ratio.

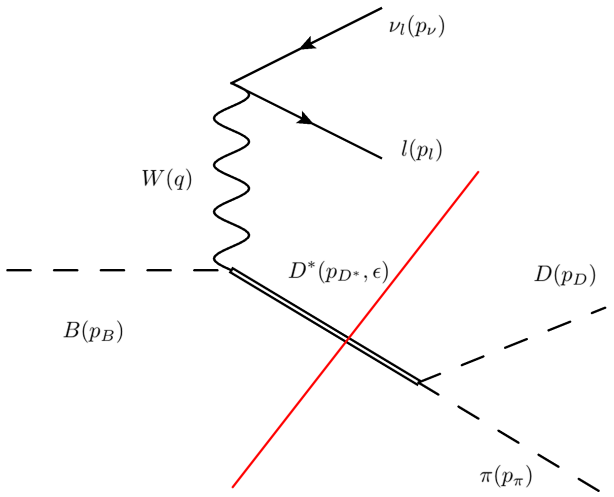

Figure 3.1: $B \to l\nu\pi D$ decay, often considered as subsequent but independent $B \to l\nu D^*$ and $D^* \to D\pi$ decays as illustrated by the red cutting line.

Since we have already established that the subsequent decay process can have different contributions depending on the lepton flavor, let us go one step further and consider the proper four-body decay where the D^* is allowed to be off shell. The actual amplitude for this process is

$$M = M_3^\mu D_{\mu\nu} M_2^\nu,$$

where $D_{\mu\nu}$ is the propagator of the D^*, which has the form

$$D^{\mu\nu} = \frac{-iT^{\mu\nu}}{p_{D^*}^2 - m_{D^*}^2 + im_{D^*}\Gamma(p_{D^*}^2)} + \frac{iL^{\mu\nu}}{m_{D^*}^2 - iIm\Pi_L(p_{D^*}^2)}, \tag{3.2}$$

as will be discussed in section 3.2, where $\Gamma(p_{D^*}^2)$ and $Im\Pi_L(p_{D^*}^2)$ are corrections to the vector propagator and $\Gamma(m_{D^*}^2) = \Gamma_{D^*}$ is the decay width of the D^* into $D\pi$. Because $\Gamma(p_{D^*}^2)$ is relatively small, the transversal part of the propagator has a pole close to $p_{D^*}^2 = m_{D^*}^2$ and a narrow width approximation

$$|p_{D^*}^2 - m_{D^*}^2 + im_{D^*}\Gamma(p_{D^*}^2)|^{-2} \approx \frac{\pi}{m_{D^*}\Gamma_{D^*}}\delta(p_{D^*}^2 - m_{D^*}^2)$$

can be used when integrating the squared amplitude. If we consider only the transversal part of the propagator, then the squared amplitude is

$$|M_T|^2 = M_{3\mu} M_{3\alpha}^* T^{\mu\nu} T^{\alpha\beta} M_{2\nu} M_{2\beta}^* \frac{\pi\delta(p_{D^*}^2 - m_{D^*}^2)}{m_{D^*}\Gamma_{D^*}},$$

which is exactly what one would get by squaring (3.1), plus some proportionality factors that account for the splitting of the phase space and the delta function that forces the D^* to be on shell. Therefore, using only the transversal part of the propagator is equivalent to working with the simplified model where the D^* is on shell.

However, the longitudinal part of the amplitude will remain off-shell because it lacks a pole, and introduces two new terms to the squared amplitude (one purely longitudinal and one of interference) that cannot be accounted for in the simplified model, and are what we refer to as the longitudinal corrections. In order to get a sense of the size of these corrections, we write out the form of the M_2^ν amplitude. This is simply the $D^* - D - \pi$ vertex, which must have the form of a Lorentz vector: either $(p_D + p_\pi)^\nu = p_{D^*}^\nu$ or $(p_D - p_\pi)^\nu$. If the D^* were on shell, M_2^ν would contract with ϵ_ν and so contributions proportional to $p_{D^*}^\nu$ would vanish, leaving only those proportional to $(p_D - p_\pi)^\nu$. Thus, we write $M_2^\nu = g(p_D - p_\pi)^\nu$ for some coupling constant g, and consistency with the D^* decay width requires that

$$g^2 = \frac{48\pi m_{D^*}^5 \Gamma_{D^*}}{\lambda^{3/2}(m_{D^*}^2, m_D^2, m_\pi^2)} \tag{3.3}$$

with λ as in (2.6).

Notice the slight inconsistency here: we are assuming the D^* is off shell, so we could also have a term proportional to $p_{D^*}^\nu$ in the vertex. We discuss this possibility in chapter 4, but for now we will not take it into account. The longitudinal part of the amplitude, ignoring the lower-order correction $Im\Pi_L$, is now

$$M_L = igM_3^\mu \frac{L_{\mu\nu}}{m_{D^*}^2}(p_D - p_\pi)^\nu \sim \frac{(p_{D^*})_\nu}{m_{D^*}^2}(p_D - p_\pi)^\nu = \frac{m_D^2 - m_\pi^2}{m_{D^*}^2} \equiv \Delta^2,$$

so the longitudinal term is proportional to the dimensionless mass-squared difference parameter Δ^2. This is a well-known result for any vector decaying into two pseudoscalars, and Δ^2 is usually invoked as a suppression parameter. However, due to the large $D - \pi$ mass difference, here Δ^2 has an unusually high value of 0.86, so the longitudinal corrections that are usually neglected are not heavily suppressed, and it might be no coincidence that the case of the D^* has proven the most problematic in reconciling the experimental data with the theory.

We have already written out the D^* propagator and the M_2^ν amplitude, so let us now write out the M_3^μ amplitude. Following the Feynman rules, this

can be written as

$$M_3^\mu = l^\lambda W_{\lambda\theta} V^{\theta\mu},$$

where l^λ is the leptonic charged current, $W_{\lambda\theta}$ is the propagator of the W boson, and $V^{\theta\mu}$ is the structure of the $B - D^* - W$ vertex. In the following sections, we take a closer look at each of these components in order to write out an explicit amplitude for the process.

3.2 W and D* Propagators

The propagator for the W boson is the one described in the massive case of section 2.2. Notice that the W propagator connects to two charged-current vertices, which contain the coupling constant $g/\sqrt{2}$ plus a factor of $1/2$ from the left-handed projector $\frac{1}{2}(1-\gamma_5)$. For ease of notation, we absorb into the W propagator term both couplings $g/2$ as well as the factor $1/2$ from the quark charged current but **not** from the leptonic current. Thus, the propagator is

$$W_{\lambda\theta} = \frac{g^2}{4}\left[\frac{-iT_{\lambda\theta}}{q^2 - m^2} + \frac{iL_{\lambda\theta}}{m^2}\right],$$

where q is the momentum of the W. Because the mass of the W is considerably larger compared to the center-of-mass energy of the process ($m_W \approx 80$ GeV compared to $m_B \approx 5$ GeV), we can safely take the limit $m_W^2 >> q^2$, which leaves the much simpler propagator

$$W_{\lambda\theta} = i\frac{g_{\lambda\theta}}{m_W^2} = i\sqrt{2}G_F g_{\lambda\theta}, \tag{3.4}$$

where we have defined the fermi constant

$$G_F \equiv \frac{\sqrt{2}}{8}\frac{g^2}{m_W^2} \approx 1.17 \times 10^{-5}\ \text{GeV}^{-2}.$$

The D^* is also a massive vector, so its propagator has the same form, at least to first order. This is what we refer to as the *naked propagator*,

$$D_0^{\mu\nu} = \frac{-iT_{p_{D^*}}^{\mu\nu}}{p_{D^*}^2 - m_0^2} + \frac{iL_{p_{D^*}}^{\mu\nu}}{m_0^2},$$

where we have introduced a *naked mass* parameter m_0 that need not be the physical mass of the D^*. Because the D^* can decay into other pairs and then

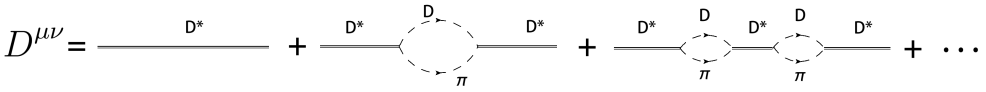

Figure 3.2: One-loop corrections to the D^* propagator.

"reassemble", we must also consider these loops in the propagator, as done in [22–24] and shown in Fig. 3.2. This is known as the one-loop correction to the propagator because it does not contain any nested loops. Here we consider only the $D\pi$ loop corrections, which is a proper assumption for the charged D^* ($BR(D^* \to D\pi) = 98\%$ [14]).

We denote the structure of the $D\pi$ loop, which must have two Lorentz indices, as $-i\Pi^{\alpha\beta}$, so that the n^{th} diagram in Fig. 3.2 can be written as

$$D_0^{\mu\alpha_1}\left(-i\Pi_{\alpha_1\beta_1}D_0^{\beta_1\alpha_2}\right)\left(-i\Pi_{\alpha_2\beta_2}D_0^{\beta_2\alpha_3}\right)\times\cdots \\ \cdots\times\left(-i\Pi_{\alpha_{n-1}\beta_{n-1}}D_0^{\beta_{n-1}\alpha_n}\right)\left(-i\Pi_{\alpha_n\beta_n}D_0^{\beta_n\nu}\right).$$

Moreover, note that the loop only depends on the momentum p_{D^*}, so $\Pi^{\alpha\beta}$ must be a combination of $p^\alpha_{D^*}p^\beta_{D^*}$ and metric tensors $g^{\alpha\beta}$, which allows us to write a decomposition in terms of the projection operators:

$$-i\Pi^{\alpha\beta} = -i\Pi_T(p^2_{D^*})T^{\alpha\beta}_{p_{D^*}} - i\Pi_L(p^2_{D^*})L^{\alpha\beta}_{p_{D^*}}.$$

Therefore, the full series for the propagator is

$$\begin{aligned} D^{\mu\nu} &= \sum_{n=0}^{\infty}\left(\frac{-iT^{\mu\alpha_1}}{p^2_{D^*}-m_0^2}+\frac{iL^{\mu\alpha_1}}{m_0^2}\right) \\ &\qquad\left[\left(-i\Pi_T T_{\alpha_1\beta_1}-i\Pi_L L_{\alpha_1\beta_1}\right)\left(\frac{-iT^{\beta_1\alpha_2}}{p^2_{D^*}-m_0^2}+\frac{iL^{\beta_1\alpha_2}}{m_0^2}\right)\right]\times\cdots \\ &\qquad\cdots\times\left[\left(-i\Pi_T T_{\alpha_n\beta_n}-i\Pi_L L_{\alpha_n\beta_n}\right)\left(\frac{-iT^{\beta_n\nu}}{p^2_{D^*}-m_0^2}+\frac{iL^{\beta_n\nu}}{m_0^2}\right)\right] \\ &= \sum_{n=0}^{\infty}\frac{-iT^{\mu\nu}}{p^2_{D^*}-m_0^2}\left(\frac{-\Pi_T}{p^2_{D^*}-m_0^2}\right)^n+\sum_{n=0}^{\infty}\frac{iL^{\mu\nu}}{m_0^2}\left(\frac{\Pi_L}{m_0^2}\right)^n, \end{aligned}$$

where in the last line we have expanded all the products while making use of the projector properties (2.3). The sums are thus reduced to simple geometric series,

$$\sum x^n = \frac{1}{1-x},$$

and the propagator is then

$$D^{\mu\nu} = \frac{-iT^{\mu\nu}}{p_{D^*}^2 - m_0^2 + \Pi_T} + \frac{iL^{\mu\nu}}{m_0^2 - \Pi_L}.$$

Notice that the real parts of the functions Π_T, Π_L are just scalars that can be absorved into the mass parameter by defining the physical mass $m_{D^*}^2 = m_0^2 - Re(\Pi)$, which is the real mass that we observe. This is in principle different for Π_T and Π_L, but we neglect this in favor of the more interesting effect of adding an imaginary quantity to the denominators. In terms of the physical mass, the propagator is

$$D^{\mu\nu} = \frac{-iT^{\mu\nu}}{p_{D^*}^2 - m_{D^*}^2 + iIm(\Pi_T)} + \frac{iL^{\mu\nu}}{m_{D^*}^2 - iIm(\Pi_L)}, \tag{3.5}$$

and the one-loop functions $Im(\Pi_T), Im(\Pi_L)$ can be explicitly computed [22–24]:

$$Im(\Pi_T) = \frac{g^2}{48\pi p_{D^*}^4}\lambda^{3/2}(p_{D^*}^2, m_D^2, m_\pi^2) \equiv \sqrt{p_{D^*}^2}\Gamma(p_{D^*}^2),$$

$$Im(\Pi_L) = -\frac{g^2\lambda^{1/2}(p_{D^*}^2, m_D^2, m_\pi^2)}{16\pi}\left(\frac{m_D^2 - m_\pi^2}{p_{D^*}^2}\right)^2,$$

where g is the same $D^* - D - \pi$ coupling defined in (3.3) and λ is defined in (2.6). When taken on shell we have $Im(\Pi_T) = m_{D^*}\Gamma_{D^*}$, as previously mentioned, and $Im(\Pi_L) \sim \Delta^4$ is a correction to the longitudinal part of second order in Δ^2 which is more suppressed but may not be negligible as already argued.

3.3 Leptonic Charged-Current Tensor

The propagator of the W boson contracts with the leptonic charged current, given by

$$l^\lambda = \frac{1}{2}\bar{u}_l\gamma^\lambda(1-\gamma_5)v_\nu,$$

where u_l and v_ν are the particle and anti-particle spinors for the charged lepton and the neutrino, respectively. Since we need to compute the squared amplitude and sum over all spins of the products, it is more convenient to work with the spin-summed leptonic tensor

$$l^{\lambda_1\lambda_2} \equiv \sum l^{\lambda_1} l^{\dagger\lambda_2} = \sum Tr\left[u_l\bar{u}_l\gamma^{\lambda_1}\frac{1}{2}(1-\gamma_5)v_\nu\bar{v}_\nu\gamma^{\lambda_2}\frac{1}{2}(1-\gamma_5)\right],$$

where the sum is over spins of l and ν, the product has been written as a trace of Dirac gamma matrices, and the ciclicity of the trace has been used. Using the spin sum rules (2.1), we can rewrite this as

$$\begin{aligned} l^{\lambda_1\lambda_2} =& Tr\left[\left(\gamma^\alpha p_{l\alpha} + m_l\right)\gamma^{\lambda_1}\frac{1}{2}(1-\gamma_5)\left(\gamma^\beta p_{\nu\beta}\right)\gamma^{\lambda_2}\frac{1}{2}(1-\gamma_5)\right] \\ =& Tr\left[\left(\gamma^\alpha p_{l\alpha} + m_l\right)\gamma^{\lambda_1}\frac{1}{2}(1-\gamma_5)\left(\gamma^\beta p_{\nu\beta}\right)\gamma^{\lambda_2}\right], \end{aligned}$$

where in the second line we have anti-commuted one of the left projectors past two gamma matrices and used the property

$$\left[\frac{1}{2}(1-\gamma_5)\right]^2 = \frac{1}{2}(1-\gamma_5).$$

The trace can now be evaluated systematically using the following Dirac trace properties:

$$\begin{gathered} Tr\left(\gamma^\mu\right) = Tr\left(\gamma_5\right) = Tr\left(\gamma^\mu\gamma_5\right) = 0, \\ Tr\left(\gamma^\mu\gamma^\nu\right) = 4g^{\mu\nu}, \qquad Tr\left(\gamma^\mu\gamma^\nu\gamma_5\right) = 0, \\ Tr\left(\gamma^\mu\gamma^\nu\gamma^\theta\right) = Tr\left(\gamma^\mu\gamma^\nu\gamma^\theta\gamma_5\right) = 0, \\ Tr\left(\gamma^\mu\gamma^\nu\gamma^\theta\gamma^\omega\right) = 4\left(g^{\mu\nu}g^{\theta\omega} - g^{\mu\theta}g^{\nu\omega} + g^{\mu\omega}g^{\nu\theta}\right), \\ Tr\left(\gamma^\mu\gamma^\nu\gamma^\theta\gamma^\omega\gamma_5\right) = -4i\epsilon^{\mu\nu\theta\omega}, \end{gathered}$$

and the end result is:

$$l^{\lambda_1\lambda_2} = -2g^{\lambda_1\lambda_2}(p_l\cdot p_\nu) + 2p_l^{\lambda_1}p_\nu^{\lambda_2} + 2p_\nu^{\lambda_1}p_l^{\lambda_2} + 2i\epsilon^{\lambda_1\lambda_2\alpha\beta}(p_l)_\alpha(p_\nu)_\beta. \tag{3.6}$$

We note that under the exchange of the indices $\lambda_1 \leftrightarrow \lambda_2$, this has a symmetric part that is real and an antisymmetric part that is imaginary:

$$\begin{aligned} l_S^{\lambda_1\lambda_2} &= -2g^{\lambda_1\lambda_2}(p_l\cdot p_\nu) + 2p_l^{\lambda_1}p_\nu^{\lambda_2} + 2p_\nu^{\lambda_1}p_l^{\lambda_2} \\ l_A^{\lambda_1\lambda_2} &= 2i\epsilon^{\lambda_1\lambda_2\alpha\beta}(p_l)_\alpha(p_\nu)_\beta \end{aligned} \tag{3.7}$$

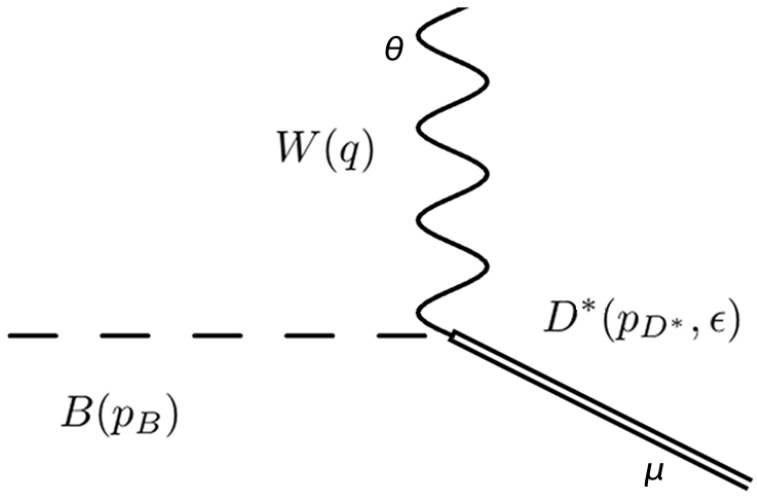

Figure 3.3: The $B - D^* - W$ vertex is shown along with the notation that we use. The indices μ, θ represent the notation for which part contracts with the D^* and which part contracts with the W.

3.4 B – D* – W Vertex

In this section we consider the structure of the vertex between the B, the D^* and the W, shown in Fig. 3.3. In this section, we adopt the notation presented in this figure. Since the $B \to D^*$ can be seen as a $b \to c$ quark transition at a first approximation, with a spectator u or d quark, the vertex should be proportional to the CKM matrix element V_{cb}, as well as the coupling $g/\sqrt{2}$ which has already been absorbed into (3.4). However, as previously discussed, the presence of strong interactions makes it unfeasible to directly compute the structure of the vertex. Instead, we must write down the most general form of the vertex and then use experimental data to approximate the particular values. Because the vertex contracts with two vector particles, it must contain two Lorentz indices, and it is a function of the two independent momenta q and p_{D^*}. There are six different Lorentz tensors that satisfy these conditions:

- $\epsilon^{\theta\mu\alpha\beta}(p_{D^*})_\alpha q_\beta$
- $q^\theta q^\mu$
- $p^\theta_{D^*} q^\mu$

- $g^{\theta\mu}$
- $q^\theta p^\mu_{D^*}$
- $p^\theta_{D^*} p^\mu_{D^*}$

The common parametrization of this vertex [2, 25, 26] considers the D^* to be on shell, so that the μ index contracts with the D^* polarization ϵ_μ and the last two terms in the list are irrelevant because $p^\mu_{D^*}\epsilon_\mu = 0$. Of course, we are taking the D^* to be off shell, so these terms should still be present. This is discussed further in section 4.4, but for now we stick to this parametrization as it is the only one available. The most general vertex that we are left with is a linear combination of four different terms, and each of them must come with a factor that may depend on the only scalar involved, which we may take as q^2 (the W is not assumed to be on shell). These scalar factors are called *form factors*, and in this case we denote them by $V(q^2)$, $A_0(q^2)$, $A_1(q^2)$ and $A_2(q^2)$. The convention is to consider the four Lorentz structures in a different basis than the one shown in the list, as follows:

$$\begin{aligned}\langle B(p_B)|\, J^\theta(q)\, |D^*(p_{D^*},\epsilon)\rangle =& V_{cb}\Bigg[\frac{2iV(q^2)}{m_B+m_{D^*}}\epsilon^{\theta\mu\alpha\beta}q_\alpha(p_{D^*})_\beta - 2m_{D^*}A_0(q^2)\frac{q^\theta q^\mu}{q^2} \\ &- (m_B+m_{D^*})A_1(q^2)\left(g^{\theta\mu}-\frac{q^\theta q^\mu}{q^2}\right) \\ &+ \frac{A_2(q^2)q^\mu}{m_B+m_{D^*}}\left((q+2p_{D^*})^\theta - \frac{m_B^2-m_{D^*}^2}{q^2}q^\theta\right)\Bigg]\epsilon_\mu\end{aligned} \tag{3.8}$$

where $J^\theta = \frac{1}{2}\bar{u}_b\gamma^\mu(1-\gamma_5)u_c$ is the charged-current for the quarks. This quantity, with the polarization ϵ_μ factored out, is what we use as the vertex structure $V_{\theta\mu}$, which in the full amplitude will contract with the D^* propagator instead of ϵ. Notice that terms proportional to $p^\mu_{D^*}$ would still vanish when contracting with the transversal part of the propagator, but not when contracting with the longitudinal part! This parametrization is chosen so that the terms accompanying A_0 and A_1 are the $L_q^{\theta\mu}$ and $T_q^{\theta\mu}$ projectors, respectively, while the A_2 term is chosen to be linearly independent to the others while still being transversal to q_θ just like $T_q^{\theta\mu}$. That is,

$$\left((q+2p_{D^*})^\theta - \frac{m_B^2-m_{D^*}^2}{q^2}q^\theta\right)q_\theta = 0$$

when p_{D^*} is on shell. The notation also reflects the fact that the V term comes from the vector part of the charged current, while the A_i terms come from the axial part of the charged current. Since $q = p_l + p_\nu$, we note that A_0 represents a longitudinal behavior of the lepton-neutrino system, whereas A_1 and A_2 represent the transversal behavior of it.

Instead of q^2, it is convenient to work with a parameter proportional to the square of the recoil hadronic velocity:

$$w \equiv 1 - \frac{1}{2}\left(\frac{p_B}{m_B} - \frac{p_{D^*}}{m_{D^*}}\right)^2 = \frac{p_B \cdot p_{D^*}}{m_B m_{D^*}} = \frac{m_B^2 + m_{D^*}^2 - q^2}{2 m_B m_{D^*}}$$

Since the b and c quarks are quite heavy, we can consider the velocity of the mesons to be dictated by theirs. Moreover, the recoil velocity tends to zero in the limit of infinite mass, so we would expect $w \approx 1$ which leads us to work with an expansion in orders of $w - 1$. This is known as a *Heavy Quark Effective Theory*, and it can be used to provide a parametrization of the form factors. The usual approach is to define A_1 in terms of a universal form factor

$$h_{A_1}(w) = \frac{A_1(q^2)}{R_{D^*}} \frac{2}{w+1}$$

with $R_{D^*} \equiv 2\sqrt{m_B m_{D^*}}/(m_B + m_{D^*})$, and then define the other form factors in terms of ratios R_0, R_1, R_2:

$$V(q^2) = R_1(w)\frac{h_{A_1}}{R_{D^*}},$$

$$A_0(q^2) = R_0(w)\frac{h_{A_1}}{R_{D^*}},$$

$$A_2(q^2) = R_2(w)\frac{h_{A_1}}{R_{D^*}}.$$

The result of the HQET calculation is [2, 25, 26]:

$$\begin{aligned}
&R_1(w) = R_1(1) - 0.12(w-1) + 0.05(w-1)^2, \\
&R_0(w) = R_0(1) - 0.11(w-1) + 0.01(w-1)^2, \\
&R_2(w) = R_2(1) + 0.11(w-1) - 0.06(w-1)^2, \text{ and} \\
&h_{A_1}(w) = h_{A_1}(1)\left[1 - 8\rho^2 z + (53\rho^2 - 15)z^2 - (231\rho^2 - 91)z^3\right], \\
&\text{with } z \equiv \frac{\sqrt{w+1} - \sqrt{2}}{\sqrt{w+1} + \sqrt{2}},
\end{aligned} \tag{3.9}$$

Table 3.1: Input values used for our calculation have been taken from Belle results [27]. For completeness, we also show the world-average results computed by HFLAV[12].

	Belle	Average
$h_{A_1}(1)\lvert V_{cb}\rvert$	$(34.6 \pm 0.2 \pm 1.0) \times 10^{-3}$	$(35.61 \pm 0.43) \times 10^{-3}$
ρ^2	$1.214 \pm 0.034 \pm 0.009$	1.205 ± 0.026
$R_1(1)$	$1.401 \pm 0.034 \pm 0.018$	1.404 ± 0.032
$R_2(1)$	$0.864 \pm 0.024 \pm 0.008$	0.854 ± 0.020

which has five free parameters $R_1(1), R_0(1), R_2(1), h_{A_1}(1), \rho^2$ that must be measured experimentally. For our calculations we use the results obtained by Belle [27] for $R_1(1), R_2(1), h_{A_1}(1), \rho^2$ using $B \to l\nu D^*$ decays for the light flavors, shown in Table 3.1, which are in agreement with world-average measurements [12]. The parameter $R_0(1)$ cannot be extracted from these decays for reasons discussed in section 4.3, so instead we make use of another identity derived [2, 25, 28] from HQEFT:

$$\frac{R_2(1)(1 - m_{D^*}/m_B) + (m_{D^*}/m_B)\left[R_0(1)(1 + m_{D^*}/m_B) - 2\right]}{(1 - m_{D^*}/m_B)^2} = 0.97 \quad (3.10)$$

to derive $R_0(1)$ in terms of $R_2(1)$.

We have now fully described all elements of the $B \to l\nu\pi D$ decay, whose full squared amplitude can be written as

$$|M|^2 = 2G_F^2 l^{\lambda_1\lambda_2} V_{\lambda_1\mu_1} V^*_{\lambda_2\mu_2} D^{\mu_1\nu_1} \left(D^{\mu_2\nu_2}\right)^* g^2 (p_D - p_\pi)_{\nu_1} (p_D - p_\pi)_{\nu_2},$$

and are ready to proceed with the integration as described in section 2.6. The results will be discussed in the following chapter.

Chapter 4

Discussion on the $R_{D\pi}$ Ratio

In this section we present the main results of this work as well as the discussion on them. We begin by providing our numerical calculation for the $R_{D\pi}$ ratio in section 4.1, and then elaborate further on the origin and form of the interference term of the amplitude in section 4.2. The remaining sections are dedicated to laying a groundwork for other aspects that should be considered for future research on this topic, and which could potentially further refine our value of $R_{D\pi}$: in section 4.3 we discuss the importance of a direct measurement of the A_0 form factor, and in section 4.4 we consider the presence of additional form factors in the QCD vertex as well as additional resonances for the $D\pi$ mass distribution. Section 4.5 presents various other minor considerations that we have considered worth noting.

4.1 Calculation of the $R_{D\pi}$ ratio

As mentioned in chapter 3, the squared amplitude for the $B \to l\nu\pi D$ process consists of three terms: transversal, longitudinal, and interference. In the notation of section 3.1, the interference term is

$$|M|_I^2 = \frac{M_3^{\mu_1} M_3^{*\mu_2} M_2^{\nu_1} M_2^{*\nu_2}}{p_{D^*}^2 - m_{D^*}^2 + i m_{D^*}\Gamma(p_{D^*}^2)} \left(\frac{T_{\mu_1\nu_1} L_{\mu_2\nu_2} + L_{\mu_1\nu_1} T_{\mu_2\nu_2}}{m_{D^*}^2 + iIm\Pi_L} \right),$$

and we can implement the narrow width approximation by writing

$$\frac{1}{p^2_{D^*} - m^2_{D^*} + im_{D^*}\Gamma(p^2_{D^*})} = \frac{p^2_{D^*} - m^2_{D^*} - im_{D^*}\Gamma(p^2_{D^*})}{|p^2_{D^*} - m^2_{D^*} + im_{D^*}\Gamma(p^2_{D^*})|^2}$$

$$\begin{aligned} &\approx \left(p^2_{D^*} - m^2_{D^*} - im_{D^*}\Gamma(p^2_{D^*})\right) \frac{\pi\delta(p^2_{D^*} - m^2_{D^*})}{m_{D^*}\Gamma} \\ &= -i\pi\delta(p^2_{D^*} - m^2_{D^*}), \end{aligned}$$

where the last step is valid inside the integral by invoking the $p^2_{D^*} = m^2_{D^*}$ condition enforced by the delta function. Therefore, the transversal, interference and longitudinal terms are:

$$\begin{aligned} |M|^2_T &= |M^\mu_3 T_{\mu\nu} M^\nu_2|^2 \frac{\pi}{m\Gamma_{D^*}} \delta(p^2_{D^*} - m^2_{D^*}) \\ |M|^2_I &= -iM^{\mu_1}_3 M^{*\mu_2}_3 M^{\nu_1}_2 M^{*\nu_2}_2 \left(\frac{T_{\mu_1\nu_1}L_{\mu_2\nu_2} + L_{\mu_1\nu_1}T_{\mu_2\nu_2}}{m^2_{D^*} + iIm\Pi_L}\right) \pi\delta(p^2_{D^*} - m^2_{D^*}) \\ |M|^2_L &= |M^\mu_3 L_{\mu\nu} M^\nu_2|^2 \frac{1}{m^4_{D^*} + (Im\Pi_L)^2}. \end{aligned} \tag{4.1}$$

As already mentioned, the transversal term exhibits a delta function that forces the D^* to be on shell while the longitudinal term does not. Although the longitudinal term has no delta function, it should also be integrated around $p^2_{D^*} \approx m^2_{D^*}$ because the experiments select only the processes with a $p_D + p_\pi$ momentum close to the D^* resonance. For our calculation we have chosen to integrate this over $p^2_{D^*} \in m^2_{D^*} \pm \delta$, with δ ranging from $\Gamma_{D^*}/2$ to 1 MeV but, as expected, the lack of a pole makes the integration over this small region negligible. The interference term, however, inherits the pole from the transversal part of the propagator which can again be approximated to a delta function. It is in this way that the longitudinal degree of freedom, upon interference with the transversal one, introduces a correction even when evaluated on shell, and we have found this contribution to be sizable.

We have also found that the interference term makes a slight distinction between the $l = e$ and $l = \mu$ cases. Thus, we quote our final result separately as

$$R^e_{D\pi} = 0.271 \pm 0.003$$

and

$$R^\mu_{D\pi} = 0.273 \pm 0.003,$$

where the uncertainty comes from the uncertainties on the measurement [27] of the form factor parameters discussed in section 3.4. Notice that the relationship (3.10) between A_0 and A_2 introduces an anti-correlation on the form factors, which brings the uncertainties lower.

In Table 4.1, we show the contribution to the branching ratio from the transversal, longitudinal (with $\delta = \Gamma_{D^*}/2$) and interference parts of the amplitude for all three lepton flavor products, which are consistent with Belle measurements for the electron and muon [27]. Within parenthesis we quote the errors coming from the uncertainties in the form factor parameters and V_{cb} [27]. In the last two rows we show $R_{D\pi}$ for the electron and the muon as each part is added subsequently from left to right. As expected, taking only the transversal part replicates the $R_{D^*} = 0.252$ result [2], while the longitudinal part itself introduces a negligible correction. However, the interference part introduces a sizable correction that creates a sharp difference between $R_{D\pi}$ and R_{D^*}. In Table 4.2 we also plot the value of the longitudinal contribution as the integration interval parameter δ is increased from $\Gamma_{D^*}/2$ to 1 MeV to show that, although the contribution increases with δ, it remains negligible throughout, so the choice of this parameter is unimportant.

Notice that, due to the cancellation of global factors in the ratio (mainly V_{cb} and $h_{A_1}(1)$), $R_{D\pi}$ has a much higher precision than the individual branching ratios. Comparing with $R_{D\pi}$ instead of R_{D^*} improves the agreement with the experiments in all cases. In particular, the gap with the latest LHCb results [8, 9] goes down from 1.1 σ to 0.48 σ, while the gap with the latest Belle results [10, 11] goes from 0.42 σ to 0.10 σ, and with the world average [12] from 3.7 σ to 2.1 σ.

The longitudinal degree of freedom has been considered before as a correction to R_{D^*} by a few authors, but the interference has not been contemplated. In [2], the transversal and longitudinal contributions are considered separately and a ratio for the purely longitudinal contributions of $R^L_{D^*} = 0.115(2)$ is found, in agreement with our result of 0.111(3) when integrated over the whole phase space (which is not what is shown in the table), but the interference is not computed. In [29], the complete four-body amplitude is considered but the interference is found to be negligible. This can be traced back to the propagator being used, which effectively differs from the one here by a factor of $(p^2_{D^*} - m^2_{D^*})/(p^2_{D^*} - m^2_{D^*} + im_{D^*}\Gamma_{D^*})$ in the longitudinal part which makes it vanish when evaluated on shell (as is the case in the interference).

In our case, we have found that the longitudianl corrections, through the

Table 4.1: Contribution to the branching ratio of the transversal, longitudinal and interference parts of the amplitude for all three lepton flavors. The longitudinal part has been integrated over $p^2_{D^*} = m^2_{D^*} \pm \Gamma_{D^*}/2$. Quantities are given in percentage. The last two rows show the value of $R_{D\pi}$ as each contribution is added subsequently from left to right for e and μ.

	Transversal	Longitudinal	Interference
Electron	4.6(3)	$2.5(2) \times 10^{-6}$	$7.6(6) \times 10^{-8}$
Muon	4.6(3)	$2.5(2) \times 10^{-6}$	$1.6(1) \times 10^{-3}$
Tau	1.16(8)	$5.5(4) \times 10^{-7}$	$1.02(7) \times 10^{-1}$
$R^e_{D\pi}$	0.252	0.252	0.274,
$R^\mu_{D\pi}$	0.252	0.252	0.275

Table 4.2: Contribution of the purely longitudinal part of the amplitude integrated over the region $p^2_{D^*} \in m^2_{D^*} \pm \delta$ with δ ranging from $\Gamma_{D^*}/2$ to 1 MeV.

δ	$\Gamma^\tau_L(\%)$	$\Gamma^\mu_L(\%)$	$\Gamma^e_L(\%)$
$\frac{1}{2}\Gamma_{D^*}$	$5.5(4) \times 10^{-7}$	$2.5(2) \times 10^{-6}$	$2.5(2) \times 10^{-6}$
Γ_{D^*}	$1.10(6) \times 10^{-6}$	$5.0(3) \times 10^{-6}$	$5.0(3) \times 10^{-6}$
$\frac{3}{2}\Gamma_{D^*}$	$1.66(9) \times 10^{-6}$	$7.5(4) \times 10^{-6}$	$7.5(4) \times 10^{-6}$
$2\Gamma_{D^*}$	$2.2(1) \times 10^{-6}$	$1.0(6) \times 10^{-5}$	$1.0(6) \times 10^{-5}$
1 MeV	$1.33(8) \times 10^{-5}$	$6.0(3) \times 10^{-5}$	$6.0(3) \times 10^{-5}$

interference term, manage to virtually eliminate discrepancies with the latest experimental results. Although the agreement with the world average is also greatly improved, there is still some tension than cannot be explained by our results so far. In sections 4.3, 4.4 and 4.5 we discuss a few other details that could be used to further refine these results.

4.2 The Interference Term in $B \to l\nu\pi D$

Since we have argued that it is of great relevance, let us elaborate more on the form of the interference term in the $B \to l\nu\pi D$ decay process. The propagator in (3.5), when ignoring the smaller order correction Π_L and taken to be on shell, can be written as

$$D^{\mu\nu}_{on} \sim \frac{-T^{\mu\nu}}{m_{D^*}\Gamma_{D^*}} + \frac{iL^{\mu\nu}}{m^2_{D^*}}.$$

Given the relative factor of i between the two terms, it is tempting to think that the interference would vanish, but this is not the case because of the Lorentz structure. Specifically, let us write the complete squared amplitude as

$$|M|^2 = l^{\lambda_1\lambda_2}\left(H^T_{\lambda_1} + H^L_{\lambda_1}\right)\left(H^{T*}_{\lambda_2} + H^{L*}_{\lambda_2}\right), \tag{4.2}$$

where $l^{\lambda_1\lambda_2}$ is the leptonic tensor described in (3.6) and H^T_λ, H^L_λ are the hadronic part of the amplitude going through the transversal and longitudinal term of the D^* propagator, respectively. The interference term can then be written as

$$\begin{aligned} |M|^2_I =& l^{\lambda_1\lambda_2}\left(H^T_{\lambda_1}H^{L*}_{\lambda_2} + H^L_{\lambda_1}H^{T*}_{\lambda_2}\right) \\ =& 2l^{\lambda_1\lambda_2}_S Re\left(H^T_{\lambda_1}H^{L*}_{\lambda_2}\right) + 2l^{\lambda_1\lambda_2}_A Im\left(H^T_{\lambda_1}H^{L*}_{\lambda_2}\right), \end{aligned} \tag{4.3}$$

where $l^{\lambda_1\lambda_2}_S, l^{\lambda_1\lambda_2}_A$ are the symmetric and antisymetric parts of the leptonic tensor, described in (3.7). Note that , $l^{\lambda_1\lambda_2}_A$ is proportional to the Levi-Civita symbol which vanishes unless it ultimately contracts with the four independent momenta p_l, p_ν, p_{D^*}, p_D. The last one can only come from the $D^* - D - \pi$ vertex, and can only "connect" to the Levi-Civita if it contracts with one metric tensor in the D^* propagator (found only in the transversal part) and then another metric tensor in the $B - D^* - W$ vertex (found only in the term proportional to A_1 in (3.8)). Thus, the second interference term is always proportional to $A_1(q^2)$.

In order to study the other interference term, let us now write the factorization $H^T_\lambda \equiv (iV_{\lambda\mu} + A_{\lambda\mu})\, T^\mu$ and $H^L_\lambda \equiv A_{\lambda\mu} i L^\mu$, where $V_{\lambda\mu}$ and $A_{\lambda\mu}$ represent the vector and axial terms of the $B - D^* - W$ vertex in (3.8), respectively, and T^μ, L^μ represent the remaining parts of the corresponding amplitudes. We have factored an i out of $V_{\lambda\mu}$ and L^μ so that all the quantities that have been defined are real. Also, note that we have not included the $V_{\lambda\mu}$ term in the factorization for H^L_λ because the Levi-Civita term that accompanies the V form factor in (3.8) vanishes when contracted with the longitudinal projector $L^{\mu\nu}_{p_{D^*}}$. In this notation, we have

$$\begin{aligned} Re\left[H^T_{\lambda_1} H^{L*}_{\lambda_2}\right] =& Re\left[i\left(iV_{\lambda_1\mu_1} + A_{\lambda_1\mu_1}\right) T^{\mu_1} A_{\lambda_2\mu_2} L^{\mu_2}\right] \\ =& - V_{\lambda_1\mu_1} A_{\lambda_2\mu_2} T^{\mu_1} L^{\mu_2}, \end{aligned}$$

which is always proportional to the V form factor which also contains a Levi-Civita.

Thus, we obtain two interference terms: the first in (4.3) proportional to $V(q^2)$ and the second proportional to $A_1(q^2)$, and both proportional to the Levi-Civita term $|\epsilon| \equiv \epsilon_{\alpha\beta\gamma\delta} p_l^\alpha p_\nu^\beta p_{D^*}^\gamma p_D^\delta$. This term is closely related to the chirality of the lepton, which depends on its mass. If we work on the rest frame of the lepton, then

$$\begin{aligned} |\epsilon| =& m_l \epsilon_{0\beta\gamma\delta} p_\nu^\beta p_{D^*}^\gamma p_D^\delta \\ =& m_l \vec{p}_\nu \cdot (\vec{p}_{D^*} \times \vec{p}_D) \\ =& m_l |\vec{p}_\nu||\vec{p}_{D^*}||\vec{p}_D| \sqrt{1 + 2\cos\alpha\cos\beta\cos\gamma - \cos^2\alpha - \cos^2\beta - \cos^2\gamma}, \end{aligned} \tag{4.4}$$

where α, β, γ are the angles between $\vec{p}_\nu - \vec{p_{D^*}}$, $\vec{p}_\nu - \vec{p}_D$, and $\vec{p_{D^*}} - \vec{p}_D$. In this frame we see a clear dependence of the interference on the mass of the lepton, which explains why the contributions of the interference follow the same hierarchy as the masses of the leptons.

For integration purposes, the angle θ_{ij} between the momenta of particles i and j can be expressed as

$$\cos(\theta_{ij}) = \frac{-p_i \cdot p_j + E_i E_j}{\sqrt{\left(E_i^2 - m_i^2\right)\left(E_j^2 - m_j^2\right)}},$$

where $p_i \cdot p_j$ is easily expressed in terms of the scalar variables and, in the rest frame of the tau,

$$E_i = \frac{p_\tau \cdot p_i}{m_\tau}.$$

4.3 Measurement of the A_0 Form Factor

The term with the A_0 form factor in (3.8) has the form of a longitudinal projector in $q = p_l + p_\nu$, which represents the contribution with longitudinal polarization of the lepton-neutrino system. Since this state is forbidden in the limit of zero mass, the contribution of A_1 is heavily suppressed for the electron and muon, but not for the tau. This effect can be observed in Fig. 4.1, where we plot the contribution of each of the vertex terms to the squared amplitude. Notice that A_0 represents the second largest contribution for the tau, whereas for the electron it is practically absent.

This drastically different behavior between the tau and the light flavors makes A_0 a prime candidate for explaining discrepancies in the $R_{D\pi}$ ratio, which is made even more interesting by the fact that its corresponding parameter $R_0(1)$ in (3.9) has never been meassured directly. This is so because the measurements of the form factors performed by the Belle [27] and BaBar [30] collaborations have been done with data of light-flavored lepton decays, to which the A_1 contribution is unaccessible. Instead, $R_0(1)$ is calculated in terms of $R_2(1)$ using another HQEFT approximaion as described in (3.10) and plugged directly into the tau decay to estimate its contribution.

Given the relatively high contribution of A_1 to the decay into the tau and its discriminative behavior, we believe that a carefull study of the $R_0(1)$ parameter is needed in order to properly understand the $R_{D\pi}$ ratio. Therefore, we stress the importance of making a direct measurement of this parameter using data of decays into tau, which has not been done to date.

4.4 Additional Form Factors and Other Resonances for the $D-\pi$ Mass Distribution

As mentioned in section 3.4, the description of the $B-D^*-W$ vertex that we use is incomplete since it lacks terms proportional to $p^\mu_{D^*}$ that could couple to the longitudinal term of the D^* propagator. Therefore, the vertex should in principle be parametrized with the presence of another two form factors. The same is true for the $D^*-D-\pi$ vertex which, as described in section 3.1, we have taken to be proportional to the momentum difference $(p_D - p_\pi)_\nu$ but have not considered the other independent momentum, $(p_D + p_\pi)_\nu = (p_{D^*})_\nu$ that vanishes when contracted with the transversal part of the propagator but could couple to the longitudinal term.

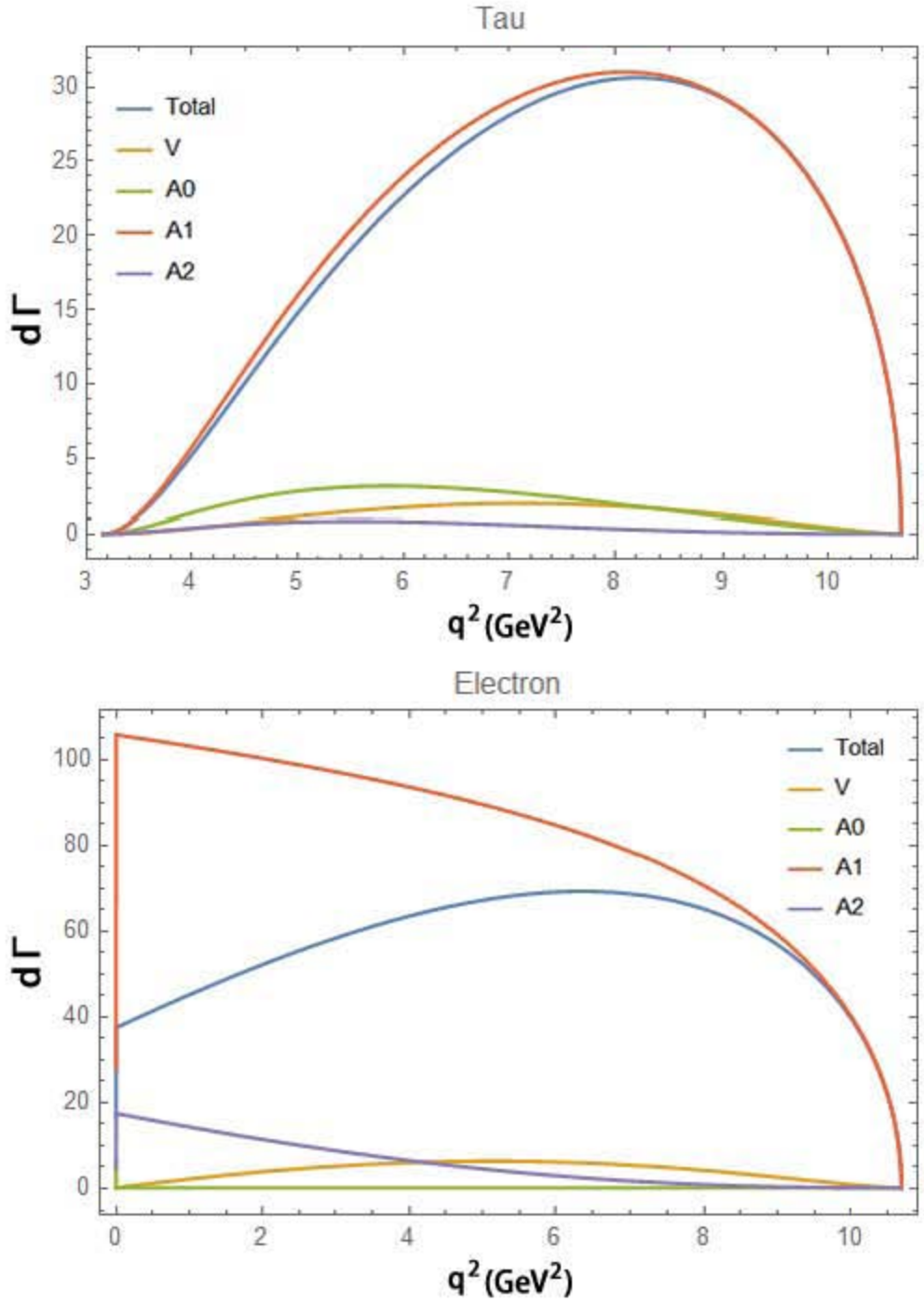

Figure 4.1: Contribution to the squared amplitude of each of the vertex form factors, plotted for the tau (top) and the electron (bottom). Notice that the A_0 contribution is heavily suppressed for the electron. Interferences between the form factors are not shown.

Rather than working with a total of 8 form factors (six for the $B-D^*-W$ vertex and two for the $D^*-D-\pi$ vertex), one can combine the information from both vertices and consider only four form factors. This is done by factoring out the leptonic current as in (4.2) so that we can write

$$M = l^\lambda H_\lambda,$$

where H_λ is the hadronic part of the amplitude. This hadronic part must be a vector and depends only on three independent momenta, which can be taken as $q_\lambda = (p_l + p_\nu)_\lambda$, $(p_{D^*})_\lambda = (p_D + p_\pi)_\lambda$ and $k_\lambda \equiv (p_D - p_\pi)_\lambda$. Thus, we can decompose H_λ into four possible terms:

$$\begin{aligned} V'_\lambda &\equiv -\frac{iV'}{m_B^3}\epsilon_{\lambda\alpha\beta\gamma}q^\alpha p_{D^*}^\beta k^\gamma \\ A'_{0\lambda} &\equiv \frac{A'_0}{m_B}q_\lambda \\ A'_{1\lambda} &\equiv \frac{A'_1}{m_B}(p_{D^*})_\lambda \\ A'_{2\lambda} &\equiv \frac{A'_2}{m_B}k_\lambda, \end{aligned} \tag{4.5}$$

so that $H_\lambda = V'_\lambda - (A'_0 + A'_1 + A'_2)_\lambda$, and where V', A'_0, A'_1, A'_2 are scalar functions. Unlike the last time, there are now three independent scalar variables (*e.g.* k^2, q^2 and $k \cdot q$) that these form factors can depend on. This type of parametrization has been used before to describe the K_{l4} decay (namely $K \to l\nu\pi\pi$) [31] in the chiral approximation, but the form factors have not been computed for the $B \to l\nu\pi D$ decay in the heavy quark approximation which presents the added complication of a large $D-\pi$ mass difference as opposed to the negligible mass difference between two pions.

In addition to new form factors, one could also consider the effect of additional resonances for the $D-\pi$ mass distribution. A recent study [29] made this consideration for the case of a B^* resonance, but found the effect on $R_{D\pi}$ to be negligible. This is due mainly to the fact that the $D-\pi$ mass distribution is only integrated over a narrow region around $m^2_{D^*}$, in compliance with experimental selection rules, so the lack of a pole near $m^2_{D^*}$ for the B^* propagator makes the contribution vanish as the integration region is made narrower. In this article, an integration region width ranging from $\Gamma^*_D/2$ to 1 MeV was used, and the B^* resonance contribution was found to remain negligible throughout. One could also consider a scalar resonance,

such as the one from $D_0^*(2400)^0$, which could mimic the longitudinal degree of freedom of the D^*. It has been shown in [22] how these scalar and longitudinal vector resonances can be described simultaneously, and an analogous calculation could be done to estimate this contribution, although we would expect it to be negligible for the same reason, namely the lack of a pole. That being said, the form factor parametrization described in (4.5) has the added advantage of describing the $B \to l\nu\pi D$ process globally, so an experimental measurement of these form factors would automatically encompass all of these effects without the need for special consideration.

4.5 Other Corrections

In this section we go over a few additional corrections that could be done for the calculation of the $R_{D\pi}$ ratio which we consider to be of lesser importance. The Belle II experiment has started recording data in early 2018, and is expected to achieve a 50-fold increase in integrated luminosity which would translate into an uncertainty for the $R_{D\pi}$ ratio only 0.57 times as big as the current one [13]. Since the experimental precision is always expected to keep improving, corrections that are currently consider small may become increasingly important in the future, and it will be mandatory to have a theoretical value to compare to that is more rigorous each time.

The form factors that describe the $B - D^* - W$ vertex, shown in (3.9), have been calculated using HQEFT to first order in the inverse mass of the b quark. Second order corrections have been calculated for this decay, and could be expected to modify the results for the branching ratios by an order up to few percent [26] which could likely become relevant in the future. It is also valuable to have available other calculations for the form factors that rely on models different than HQEFT, particularly on lattice QCD. So far, lattice QCD has been used to provide measurements on the A_1 form factor [32, 33], which have been found to be in agreement with the HQEFT calculation. However, since this form factor is used for the normalization of all the others, it enters in the branching ratio as a global factor and plays no role in the $R_{D\pi}$ ratio. In fact, the purpose of these calculations has been to extract the V_{cb} matrix element from the information of the overall factor; not to verify the HQEFT calculations.

As mentioned in the introduction, our study considers only the $D^* \to D\pi$ detection modes which is an excellent approximation for the charged D^*

case, but for a neutral D^* one would also need to make calculations for the $D^* \to D\gamma$ mode. The later case also exhibits radiate corrections which have been studied before and have been found to be relevant at the few percent level [34, 35]. For this reason, we argue that measurements with charged D^* mesons should be favored as they present a cleaner theoretical description. However, when considering the full $B \to l\nu\pi D$ decay one needs to account for radiative corrections of the daughter particles even for the case of a charged D^*. These have been studied for the case where the B decays directly into a scalar D [36], and the effect on the analogous ratio R_D has been found to be non-negligible for both the charged and uncharged cases. Therefore, it may be important to calculate radiative corrections in the full $B \to l\nu\pi D$ decay as well.

Chapter 5

Concluding Remarks

We have argued that the experimental results for the semileptonic decays $B \to l\nu D^* \to l\nu\pi D$ should be compared to theoretical quantities computed with the full four-body decay, where the D^* becomes a virtual particle and gains a longitudinal degree of freedom. Although the longitudinal term by itself lacks any contribution with a pole near the mass shell, the interference that it creates with the transversal part introduces a sizable correction. Moreover, this correction was found to be largely dependent on the lepton mass, contrary to the common belief that the the $D^* \to D\pi$ can be considered an independent subsequent process that cancels out in the ratio. In particular, this results in the fraction of branching ratios

$$R_{D\pi} = 0.274 \pm 0.003$$

as opposed to the ratio

$$R_{D^*} = 0.252 \pm 0.003$$

that is usually considered. We note that these numbers are incompatible at a statistical significance of 7.3 σ, and so choosing the right value to compare with is bound to be crucial once the experimental uncertainties start getting closer to the theoretical ones. Even at the current level of experimental precision [12], the difference between these numbers already represents the closing of a gap by 1.5 σ, and we expect this to be an even more relevant factor once the Belle 2 experiments starts taking measurements, which are expected to have a 75% increase in precision [13].

So far, the use of $R_{D\pi}$ completely eliminates any statistically significant gap with the latest Belle [10, 11] and LHCb [8, 9] results, and helps reduce the

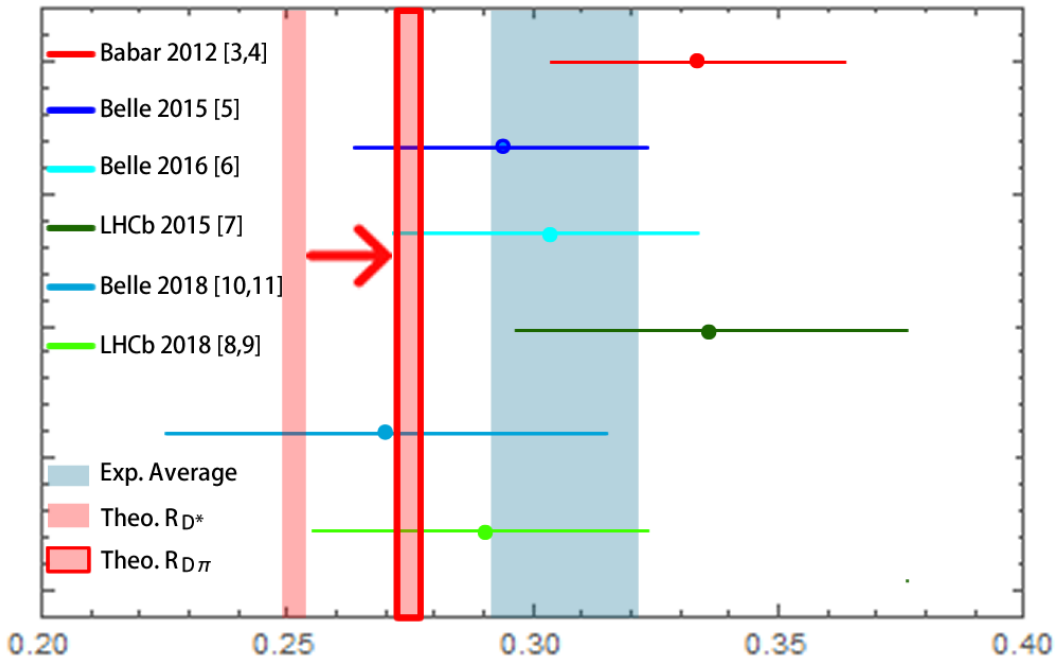

Figure 5.1: Current status of measurements for R_{D^*}. This work argues that results must actually be compared with $R_{D\pi}$ (outlined red area) as opposed to R_{D^*} (not outlined), which significantly improves the agreement.

overall gap with the world average measurements from 3.7 σ to 2.1 σ. Current measurements are shown in Fig. 5.1, along with a graphical representation of the improvement of using $R_{D\pi}$ over R_{D^*}. Although some tension still remains with the world average, we believe that this consideration alone has already greatly contributed to closing the gap on the R_{D^*} problem, and that it is now entirely in the realm of possibility that this discrepancy be resolved without the need of any lepton flavor universality violation or other forms of physics beyond the standard model. We have tried to lay a groundwork for future theoretical research on this topic, including ways in which the $R_{D\pi}$ ratio could be further refined to possibly close the gap even further. Specifically, we have proposed the following considerations:

- The direct experimental measurement of the A_0 form factor from tau-flavored decays, since this is currently indirectly inferred from light-flavored decays where it is absent despite being the second largest contribution to the tau-flavored one.
- A new analysis of Belle data [27] with the consideration of additional form factors in both the $B - D^* - W$ and $D^* - D - \pi$ vertices that could couple to the longitudinal part of the off-shell D^*.
- Additional resonances for the $D - \pi$ mass distribution, which may be vectorial or scalar.
- Alternatively to the last three points, we have also proposed the use of a global form factor parametrization for the full $B \to l\nu\pi D$ decay, like the one already in use for the case of K_{l4} [31].
- The use of lattice QCD calculations to verify the HQEFT approximations.
- Absorptive corrections that may be present when considering the daughter $D\pi$ particles.

In addition, we have also argued that the ratio obtained from neutral B mesons may be considerably different than the one obtained from charged ones, even though some experiments [3–5, 10, 11] have used both indistinctly. This is so because the longitudinal corrections we have computed apply only for the $D^* \to D\pi$ detection mode but not the $D^* \to D\gamma$ mode that is also exhibited in the case of a neutral D^* (charged B). Therefore, it is preferable

to consider neutral B decays which exhibit $D^* \to D\pi$ practically as their only mode.

Finally, we conclude by pointing out that some works have also proposed the study of the $B \to l\nu D^*$ decay through its helicity amplitudes, which corresponds to indirectly accounting for the longitudinal term of the D^* propagator in its separate amplitude. It has been proposed that direct measurements of helicity amplitudes can be used to evaluate the consistency of new physics interactions [37]. More recently, it has been shown [38] that some combinations of helicity amplitudes are strictly independent of the lepton mass, so that the standard model prediction for their ratios between different leptons is unity. A direct measurement of said combinations would provide a new way of testing for lepton flavor universality which is more efficient since the competing effect of the lepton mass is being excluded and also the theoretical result would be exact and independent of the form factors and other experimental measurements.

Bibliography

[1] H. Na, C. M. Bouchard, G. P. Lepage, C. Monahan, and J. Shigemitsu (HPQCD), Phys. Rev. **D92**, 054510 (2015), [Erratum: Phys. Rev.D93,no.11,119906(2016)].

[2] S. Fajfer, J. F. Kamenik, and I. Nisandzic, Phys. Rev. **D85**, 094025 (2012).

[3] J. P. Lees *et al.* (BABAR Collaboration), Phys. Rev. Lett. **109**, 101802 (2012).

[4] J. P. Lees *et al.* (BaBar), Phys. Rev. **D88**, 072012 (2013).

[5] M. Huschle *et al.* (Belle), Phys. Rev. **D92**, 072014 (2015).

[6] Y. Sato *et al.* (Belle), Phys. Rev. **D94**, 072007 (2016).

[7] R. Aaij *et al.* (LHCb), Phys. Rev. Lett. **115**, 111803 (2015), [Erratum: Phys. Rev. Lett.115,no.15,159901(2015)].

[8] R. Aaij *et al.* (LHCb Collaboration), Phys. Rev. Lett. **120**, 171802 (2018).

[9] R. Aaij and Aothers (LHCb Collaboration), Phys. Rev. D **97**, 072013 (2018).

[10] S. Hirose *et al.* (Belle Collaboration), Phys. Rev. Lett. **118**, 211801 (2017).

[11] S. Hirose *et al.* (Belle), Phys. Rev. **D97**, 012004 (2018).

[12] H. Amhis, Y. *et al.* (HFLAV), Eur. Phys. J. C **77**, 895 (2017), updated information available from `https://hflav-eos.web.cern.ch/hflav-eos/semi/summer18/RDRDs.html`.

[13] J. Martínez-Ortega, Journal of Physics: Conference Series **912**, 012006 (2017).

[14] K. A. Olive *et al.* (Particle Data Group), Chin. Phys. **C38**, 090001 (2014).

[15] S. Weinberg, *The Quantum Theory of Fields*, Vol. 1 (Cambridge University Press, 1995).

[16] H. Weyl, Annalen der Physik **364**, 101 (1919).

[17] D. J. Griffiths, *Introduction to elementary particles; 2nd rev. version*, Physics textbook (Wiley, New York, NY, 2008).

[18] M. Gell-Mann, Phys. Rev. **125**, 1067 (1961).

[19] A. Bhol, EPL (Europhysics Letters) **106**, 31001.

[20] R. Dutta and N. Rajeev, Phys. Rev. **D97**, 095045 (2018).

[21] R. Kumar, Phys. Rev. **185**, 1865 (1969).

[22] L. A. J. Pérez and G. T. Sánchez, Journal of Physics G: Nuclear and Particle Physics **44**, 125003 (2017).

[23] G. Lopez Castro and G. Toledo Sanchez, Phys. Rev. **D61**, 033007 (2000).

[24] M. Beuthe, R. Gonzalez Felipe, G. Lopez Castro, and J. Pestieau, Nucl. Phys. **B498**, 55 (1997).

[25] M. Neubert, Phys. Rev. D **46**, 2212 (1992).

[26] A. F. Falk and M. Neubert, Phys. Rev. D **47**, 2965 (1993).

[27] W. Dungel *et al.* (Belle), Phys. Rev. **D82**, 112007 (2010).

[28] I. Caprini, L. Lellouch, and M. Neubert, Nuclear Physics B **530**, 153 (1998).

[29] C. S. Kim, G. Lopez-Castro, S. L. Tostado, and A. Vicente, Phys. Rev. D **95**, 013003 (2017).

[30] B. Aubert *et al.* (BABAR Collaboration), Phys. Rev. D **77**, 032002 (2008).

[31] J. Bijnens, G. Colangelo, G. Ecker, and J. Gasser, in *2nd DAPHNE Physics Handbook:315-389* (1994) pp. 315–389, arXiv:hep-ph/9411311 [hep-ph] .

[32] J. Harrison, C. T. H. Davies, and M. Wingate (HPQCD Collaboration), Phys. Rev. D **97**, 054502 (2018).

[33] J. A. Bailey *et al.* (Fermilab Lattice and MILC Collaborations), Phys. Rev. D **89**, 114504 (2014).

[34] F. U. Bernlochner and H. Lacker, (2010), arXiv:1003.1620 [hep-ph] .

[35] Tostado, S. L. and Castro, G. López, Eur. Phys. J. C **76**, 495 (2016).

[36] S. de Boer, T. Kitahara, and I. Nišandžić, Phys. Rev. Lett. **120**, 261804 (2018).

[37] M. Tanaka and R. Watanabe, Phys. Rev. D **87**, 034028 (2013).

[38] T. D. Cohen, H. Lamm, and R. F. Lebed, Phys. Rev. D **98**, 034022 (2018).